Electronic Supplementary Information (ESI)

Substituent Steric Effect Boosting Phosphorescent Efficiency of $PtCu_2$ Complexes

Zhao-Yi Wang,[a,b] Jin-Yun Wang,[a,*] Li-Yi Zhang,[a] Ming Yang,[a] Xu Zhang,[a] and Zhong-Ning Chen[a,b,*]

[a] *State Key Laboratory of Structural Chemistry, Fujian Institute of Research on the Structure of Matter, Chinese Academy of Sciences, Fuzhou, Fujian 350002, China*

[b] *ShanghaiTech University, 393 Middle Huaxia Road, Pudong, Shanghai, 201210, China*

E-mail: czn@fjirsm.ac.cn

Experimental Section

General Procedures and Materials. All operations were conducted under a dry argon atmosphere using standard Schlenk techniques and vacuum-line systems unless otherwise specified. The solvents were dried, distilled, and degassed prior to use except that those for spectroscopic measurements were of spectroscopic grade. Bis(diphenylphosphinomethyl)phenylphosphine (dpmp) was prepared by synthetic procedures described in literatures.

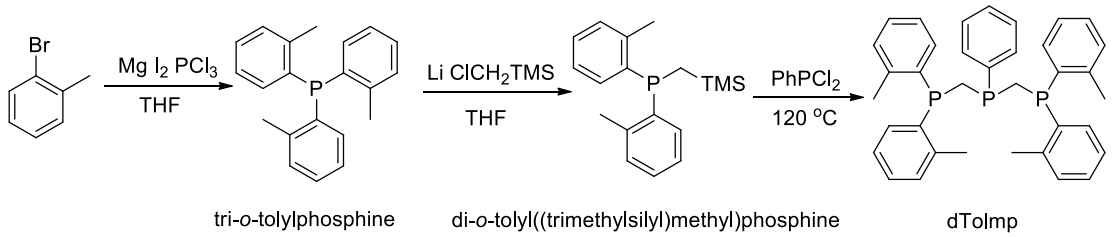

tri-*o*-tolylphosphine di-*o*-tolyl((trimethylsilyl)methyl)phosphine dTolmp

A 250 mL Schlenk flask was charged with argon, magnesium (100 mmol) and a grain of I_2 was added into THF (125 mL), a solution of 2-bromotoluene (105 mmol) added dropwise and stirred for 2.5 h at room temperature. Then the solution was cooled to -40℃, PCl_3 (33mmol) was added dropwise to the stirred Grignard solution at -40℃**,** and the reaction mixture kept at this temperature for 0.5 h, the cooling bath was removed and the mixture stirred for 5 h. A little EtOH was added and the solution was concentrated under reduced pressure, EtOH (100 mL) was added to the mixture and stirred 0.5 h, the reaction mixture was filtered and the solid was washed with EtOH three times to obtain pure product tri-o-tolylphosphine. Yield: 75%.

To a solution of tri-o-tolylphosphine (50 mmol) in dry THF, lithium turnings (150 mmol) were added in argon atmosphere, and the reaction mixture was stirred at room temperature for 1 d, lithium was separated by vacuum filtration. Then the solution was cooled at -30℃**,** chloromethyltrimethylsiane (75 mmol) was added slowly and the reaction mixture was stirred at -30℃ for 0.5 h, the cooling bath was removed and the mixture stirred at room temperature for 8 h. The solution was concentrated to dryness under reduced pressure. The crude product of di-o-tolyl((trimethylsilyl)methyl)phosphine was obtained by flash column chromatography in a vacuum and subsequently dried for 3h under vacuum. Dichlorophenylphosphine (20 mmol) was added into di-o-tolyl((trimethylsilyl)methyl)phosphine

without any solvent in Schlenk flask, and the mixture was heated at 120℃ for 5 h. After completion of the reaction, the mixture was purified by silica gel column chromatography to obtain bis(di-o-tolylphosphinomethyl)phenylphosphine (dTolmp). Yield: 70%. ^{1}H NMR ($CDCl_3$, ppm): 7.53-7.49 (m, 2H), 7.30-7.04 (m, 19H), 2.52 (d, 2H), 2.42 (d, 2H), 2.33 (s, 6H), 2.26 (s, 6H). ^{13}C NMR ($CDCl_3$, ppm): 142.33 (m), 138.95 (m), 137.20 (m), 132.56 (s), 132.35 (s), 131.66 (s), 131.34 (s), 129.98 (m), 129.16 (s), 128.56 (s), 128.44 (s), 128.28 (s), 128.20 (s), 126.04 (s), 125.93 (s), 28.96 (m), 21.31 (m). ^{31}P NMR ($CDCl_3$, ppm): -34.81 (t, 1P), -43.78 (d, 2P).

Table S1. Crystallographic Data of $PtCu_2$ Complexes **1a**–**4a**

	1a·$2CH_2Cl_2$	**2a**·$2CH_2Cl_2$	**3a**·$2CH_2Cl_2$	**4a**·$2CH_2Cl_2$·H_2O
empirical formula	$C_{86}H_{68}Cl_6Cu_2F_{12}O_8P_6Pt$	$C_{82}H_{72}Cl_6Cu_2O_8P_6Pt$	$C_{86}H_{80}Cl_6Cu_2O_{12}P_6Pt$	$C_{86}H_{84}Cl_6Cu_2N_2O_9P_6Pt$
formula weight	2178.09	1906.08	2026.19	2010.24
crystal system	monoclinic	monoclinic	triclinic	triclinic
space group	$P2_1/c$	$C2/c$	$P\bar{1}$	$P\bar{1}$
a (Å)	15.3395(5)	24.0187(12)	11.9251(13)	11.6903(9)
b (Å)	18.6529(6)	15.3260(7)	13.5254(15)	14.2170(12)
c (Å)	15.6094(4)	21.7271(11)	14.8460(17)	14.9644(13)
α (deg)			96.813(4)	63.819(3)
β (deg)	90.0800(10)	90.117(2)	108.607(4)	77.097(3)
γ (deg)			108.918(4)	89.338(3)
V (Å^3)	4466.3(2)	7998.0(7)	2079.9(4)	2164.8(3)
Z	2	4	1	1
ρ_{calcd} (g cm^{-3})	1.620	1.583	1.618	1.542
μ (mm^{-1})	2.400	2.647	2.554	2.451
radiation (λ, Å)	0.71073	0.71073	0.71073	0.71073
temperature (K)	100	100	100	100
GOF	1.054	1.118	1.069	1.053
R1 (F_o)[a]	0.0373	0.0312	0.0462	0.0251
wR2 (F_o^2)[b]	0.0961	0.0733	0.1129	0.0614

[a] $R1 = \Sigma|F_o - F_c|/\Sigma F_o$ [b] $wR2 = \Sigma[w(F_o^2 - F_c^2)^2]/\Sigma[w(F_o)^2)]^{1/2}$

Table S2. Crystallographic Data of $PtCu_2$ Complexes **1b**–**4b**

	1b	**2b**·1.95CH_2Cl_2	**3b**·1.5CH_2Cl_2·H_2O	**2b**·2CH_2Cl_2
empirical formula	$C_{96}H_{84}Cl_4Cu_2F_{18}O_6P_6PtS_2$	$C_{90.08}H_{88.03}C_{l5.9}Cu_2O_8P_6Pt$	$C_{93.5}H_{97}Cl_5Cu_2O_{13}P_6Pt$	$C_{94}H_{98}Cl_6Cu_2N_2O_8P_6Pt$
formula weight	2389.54	2015.85	2113.95	2104.43
crystal system	triclinic	monoclinic	triclinic	monoclinic
space group	$P\bar{1}$	*C*/2c	$P\bar{1}$	$P2_1/c$
a (Å)	13.1851(10)	23.5015(16)	13.8346(7)	13.4543(10)
b (Å)	14.4771(12)	18.2997(13)	15.7433(6)	15.1665(11)
c (Å)	14.8154(13)	40.788(3)	25.3399(12)	23.1761(19)
α (deg)	112.188(3)		77.505(2)	
β (deg)	94.910(3)	93.288(3)	83.276(2)	93.196(3)
γ (deg)	107.378(3)		67.421(2)	
V (Å^3)	2435.3(4)	17513(2)	4971.8(4)	4721.8(6)
Z	1	8	2	2
ρ_{calcd} (g cm^{-3})	1.629	1.529	1.412	1.480
μ (mm^{-1})	2.204	2.420	2.115	2.250
radiation (λ, Å)	0.71073	0.71073	0.71073	0.71073
temperature (K)	100	293	100	100
GOF	1.047	1.016	1.056	1.059
R1 (F_o)[a]	0.0528	0.0733	0.0724	0.0746
*w*R2 (F_o^2)[b]	0.1418	0.1665	0.1934	0.1826

[a] $R1 = \Sigma|F_o - F_c|/\Sigma F_o$ [b] $wR2 = \Sigma[w(F_o^2 - F_c^2)^2]/\Sigma[w(F_o)^2)]^{1/2}$

Table S3. Selected Bond Distances (Å) and Angles (°) of $PtCu_2$ Complexes **1a**–**4a**

	1a	**2a**	**3a**	**4a**
Pt1-Cu1	2.7556(5)	2.7097(4)	2.7199(6)	2.7355(4)
Pt1-P2	2.2983(10)	2.3025(9)	2.3114(11)	2.3017(7)
Pt1-C33	2.008(4)	2.010(4)	2.023(5)	2.016(3)
Cu1-P1	2.2419(14)	2.2331(10)	2.2351(12)	2.2752(8)
Cu1-P3	2.2309(12)	2.2535(10)	2.2578(13)	2.2392(8)
Cu1-C33	2.244(4)	2.257(4)	2.207(4)	2.190(3)
P2-Pt1-P2a	180.00	180.00	180.00	180.00
C33-Pt1-C33a	180.00	180.00	180.00	180.00
C33-Pt1-P2	92.50(12)	91.99(10)	89.70(13)	89.88(8)
C33-Pt1-P2a	87.50(12)	88.01(10)	90.30(13)	90.12(8)
P1-Cu1-P3	157.84(5)	156.11(4)	154.77(5)	155.55(3)
P1-Cu1-C33	92.13(11)	110.52(9)	109.12(12)	94.91(7)
P3-Cu1-C33	107.43(11)	93.24(9)	95.97(12)	109.17(7)

Table S4. Selected Bond Distances (Å) and Angles (°) of $PtCu_2$ Complexes **1b**–**4b**

	1b	**2b**	**3b**	**4b**
Pt-Cu	2.7347(7)	2.7789(10)/2.6877(10)	2.6999(9)/2.7931(10)	2.7141(12)
Pt-P	2.3139(13)	2.3042(19)/2.324(2)	2.2972(19)/2.3111(19)	2.306(2)
Pt-C	2.008(6)	2.015(8)/1.964(11)	2.021(8)/1.976(9)	2.023(8)
Cu-P	2.2563(15)	2.243(3)/ 2.243(3)	2.260(2)/2.2611(19)	2.628(4)
Cu-P#	2.2678(15)	2.237(2)/2.240(3)	2.262(3)/2.260(3)	2.256(3)
Cu-C	2.269(6)	2.165(8)	2.165(8)	2.162(8)
P-Pt-P#	180.00	176.08(7)	176.05(6) .	180.00
C-Pt-C#	180.00	170.9(7)	166.5(3)	180.00
C-Pt-P	87.08(15)	93.7(2)/86.5(3)	93.1(2)/84.7(2)	87.3(2)
C-Pt-P#	92.92(15)	83.8(2)/96.4(3)	84.4(2)/98.5(2)	92.7(2)
P-Cu-P#	154.75(7)	164.06(13)/156.80(13)	152.19(8)/163.36(9)	146.35(9)
P-Cu-C	111.39(14)	95.3(2)	96.0(2)	95.1(2)
P#-Cu-C	93.13(14)	100.5(2)	100.4(2)	115.8(2)

Table S5. Bond Distances (Å) and Angles (°) from X-Ray Crystallography and Optimized Structures in Singlet and Triplet States for $PtCu_2$ Complex **1a**

	crystal structure	ground state	triplet state
Pt-Cu	2.7556(5)	2.7197	2.6491
Pt-P	2.2983(10)	2.3372	2.3282
Pt-C	2.008(4)	2.0156	2.0165
Cu-P	2.2419(14)	2.2698	2.3155
Cu-P	2.2309(12)	2.2678	2.3002
Cu-C	2.244(4)	2.2794	2.2689
P-Pt1-P	180.00	179.99	179.90
C-Pt-C	180.00	179.99	179.90
C-Pt-P	92.50(12)	90.64	91.23
C-Pt-P	87.50(12)	89.34	88.67
P-Cu-P	157.84(5)	149.37	151.10
P-Cu-C	92.13(11)	96.23	100.73
P-Cu-C	107.43(11)	113.23	108.10

Table S6. Bond Distances (Å) and Angles (°) from X-Ray Crystallography and Optimized Structures in Singlet and Triplet States for $PtCu_2$ Complex **2a**

	crystal structure	ground state	triplet state
Pt-Cu	2.7097(4)	2.7426	2.6923/2.6863
Pt-P	2.3025(9)	2.3293	2.3194/2.3233
Pt-C	2.010(4)	2.0204	1.9655/2.0009
Cu-P	2.2331(10)	2.2660	2.2947
Cu-P	2.2535(10)	2.2776	2.2835
Cu-C	2.257(4)	2.2192	2.1422
P-Pt1-P	180.00	179.99	177.20
C-Pt-C	180.00	179.99	174.41
C-Pt-P	91.99(10)	90.95	90.40/88.63
C-Pt-P	88.01(10)	89.05	89.98/91.25
P-Cu-P	156.11(4)	150.91	158.08
P-Cu-C	110.52(9)	111.95	109.51
P-Cu-C	93.24(9)	96.20	92.40

Table S7. Bond Distances (Å) and Angles (°) from X-Ray Crystallography and Optimized Structures in Singlet and Triplet States for $PtCu_2$ Complex **3a**

	crystal structure	ground state	triplet state
Pt-Cu	2.7199(6)	2.7148	2.6554
Pt-P	2.3114(11)	2.3314	2.3182
Pt-C	2.023(5)	2.0181	1.9749
Cu-P	2.2351(12)	2.2684	2.2744
Cu-P	2.2578(13)	2.2779	2.2705
Cu-C	2.207(4)	2.2291	2.2826
P-Pt1-P	180.00	179.99	180.00
C-Pt-C	180.00	180.00	180.00
C-Pt-P	89.70(13)	87.44	88.06
C-Pt-P	90.30(13)	92.56	91.94
P-Cu-P	154.77(5)	148.40	153.06
P-Cu-C	109.12(12)	112.54	111.85
P-Cu-C	95.97(12)	97.87	95.08

Table S8. Bond Distances (Å) and Angles (°) from X-Ray Crystallography and Optimized Structures in Singlet and Triplet States for $PtCu_2$ Complex **4a**

	crystal structure	ground state	triplet state
Pt-Cu	2.7355(4)	2.7382	2.6652
Pt-P	2.3017(7)	2.3223	2.3084
Pt-C	2.016(3)	2.0216	1.9859
Cu-P	2.2752(8)	2.2794	2.2656
Cu-P	2.2392(8)	2.2676	2.2709
Cu-C	2.190(3)	2.1829	2.2523
P-Pt1-P	180.00	180.00	180.00
C-Pt-C	180.00	180.00	180.00
C-Pt-P	89.88(8)	89.25	89.42
C-Pt-P	90.12(8)	90.75	90.58
P-Cu-P	155.55(3)	149.57	153.54
P-Cu-C	94.91(7)	96.89	94.40
P-Cu-C	109.17(7)	112.37	112.04

Table S9. Bond Distances (Å) and Angles (°) from X-Ray Crystallography and Optimized Structures in Singlet and Triplet States for $PtCu_2$ Complex **1b**

	crystal structure	ground state	triplet state
Pt-Cu	2.7347(7)	2.7709	2.7893/2.7130
Pt-P	2.3139(13)	2.3400	2.3212/2.3265
Pt-C	2.008(6)	2.0140	1.9674/2.0081
Cu-P	2.2563(15)	2.2937	2.3713
Cu-P	2.2678(15)	2.3025	2.3125
Cu-C	2.269(6)	2.2916	2.1266/2.2467
P-Pt1-P	180.00	180.00	177.75
C-Pt-C	180.00	180.00	175.75
C-Pt-P	87.08(15)	87.13	88.28/87.39
C-Pt-P	92.92(15)	92.87	92.35/92.14
P-Cu-P	154.75(7)	156.39	162.11
P-Cu-C	111.39(14)	110.27	109.98/105.68
P-Cu-C	93.13(14)	93.01	92.11/85.87

Table S10. Bond Distances (Å) and Angles (°) from X-Ray Crystallography and Optimized Structures in Singlet and Triplet States for $PtCu_2$ Complex **2b**

	crystal structure	ground state	triplet state
Pt-Cu	2.7789(10)/2.6877(10)	2.8455/2.7282	2.6797/2.7334
Pt-P	2.3042(19)/2.324(2)	2.3230/2.3180	2.3216/2.3348
Pt-C	2.015(8)/1.964(11)	2.0290/2.0080	1.9783/2.0415
Cu-P	2.243(3)/2.243(3)	2.3062/2.2978	2.3224/2.3180
Cu-P	2.237(2)/2.240(3)	2.3021/2.2957	2.3110/2.3026
Cu-C	2.165(8)	2.1563	2.1080/2.1973
P-Pt1-P	176.08(7)	175.86	169.45
C-Pt-C	170.9(7)	165.45	153.16
C-Pt-P	93.7(2)/86.5(3)	93.90/88.09	92.79/85.93
C-Pt-P	96.4(3)/83.8(2)	94.38/84.59	95.94/90.18
P-Cu-P	164.06(13)/156.80(13)	167.17/144.95	159.83
P-Cu-C	95.3(2)	93.69	95.67/98.11
P-Cu-C	100.5(2)	100.69	102.12/105.69

Table S11. Bond Distances (Å) and Angles (°) from X-Ray Crystallography and Optimized Structures in Singlet and Triplet States for $PtCu_2$ Complex **3b**

	crystal structure	ground state	triplet state
Pt-Cu	2.6999(9)/2.7931(10)	2.6949/2.8551	2.6480/2.7468
Pt-P	2.2972(19)/2.3111(19)	2.3185/2.3220	2.3231/2.3291
Pt-C	2.021(8)/1.976(9)	2.0307/2.0043	2.0489/1.9741
Cu-P	2.260(2)/2.2611(19)	2.2926/2.3068	2.3122/2.3113
Cu-P	2.262(3)/2.260(3)	2.3041/2.3071	2.3157/2.3035
Cu-C	2.165(8)	2.1450	2.1895/2.1687
P-Pt1-P	176.05(6) .	176.36	171.08
C-Pt-C	166.5(3)	165.62	154.95
C-Pt-P	93.1(2)/84.7(2)	94.44/83.98	93.68/85.90
C-Pt-P	98.5(2)/84.4(2)	95.35/87.00	95.10/89.16
P-Cu-P	152.19(8)/163.36(9)	144.25/167.18	151.80/160.88
P-Cu-C	96.0(2)	93.62	98.58/94.33
P-Cu-C	100.4(2)	99.17	103.90/108.83

Table S12. Bond Distances (Å) and Angles (°) from X-Ray Crystallography and Optimized Structures in Singlet and Triplet States for $PtCu_2$ Complex **4b**

	crystal structure	ground state	triplet state
Pt-Cu	2.7141(12)	2.7128/2.8104	2.7148/2.6385
Pt-P	2.306(2)	2.3110/2.3222	2.3144/2.3312
Pt-C	2.023(8)	2.0386/2.0063	2.0212/1.9861
Cu-P	2.628(4)	2.3108/2.3253	2.3025/2.3122
Cu-P	2.256(3)	2.3021/2.2996	2.3178/2.3073
Cu-C	2.162(8)	2.3132/2.1090	2.1808/2.2704
P-Pt1-P	180.00	175.50	169.78
C-Pt-C	180.00	164.19	158.65
C-Pt-P	87.3(2)	87.27/84.54	88.32/86.47
C-Pt-P	92.7(2)	95.50/93.91	95.41/93.58
P-Cu-P	146.35(9)	147.44/164.31	155.17/159.06
P-Cu-C	95.1(2)	100.46/96.12	96.00/98.21
P-Cu-C	115.8(2)	109.76/99.13	106.34/101.42

Table S13. The Partial Molecular Orbital Compositions (%) by SCPA Approach (C-Squared Population Analysis Proposed by Ros and Schuit) in the Ground State and Absorption Transitions for Complex **1a** in the CH_2Cl_2 Solution Calculated by TD-DFT Method at the PBE1PBE Level.

orbital	energy (eV)	MO contribution (%)			
		Pt (s/p/d)	Cu (s/p/d)	dpmp	C≡C$C_6H_3(CF_3)_2$-2,4
LUMO+2	-1.93	6.64 (0/100/0)	8.55 (39/54/7)	51.27	33.54
LUMO+1	-2.21	12.87 (27/0/73)	5.12 (54/37/9)	25.82	56.19
LUMO	-2.89	11.04 (0/100/0)	7.78 (29/55/15)	45.65	35.53
HOMO	-6.93	15.36 (8/0/92)	20.01 (18/9/73)	17.74	46.90
HOMO-1	-7.12	25.01 (18/0/82)	38.44 (12/5/82)	30.38	6.16
HOMO-2	-7.18	1.82 (0/100/0)	39.54 (27/6/67)	28.24	30.40
HOMO-4	-7.53	13.22 (1/0/99)	21.44 (2/16/81)	45.68	19.66
HOMO-5	-7.69	11.66 (2/0/98)	3.34 (4/30/66)	61.87	23.13

state	*E*, nm (eV)	O.S.	transition (contrib.)	assignment	measured (nm)
S_1	388 (3.19)	0.3350	HOMO→LUMO (95%)	^{1}IL/^{1}MC/^{1}MLCT/^{1}LLCT	386
S_2	370 (3.35)	0.3986	HOMO-1→LUMO (94%)	^{1}MLCT/^{1}IL/^{1}MC	
S_4	341 (3.64)	0.1053	HOMO-4→LUMO (70%)	^{1}IL/^{1}MC/^{1}MLCT	
S_9	302 (4.11)	0.5438	HOMO→LUMO+2 (44%)	^{1}IL/^{1}MLCT/^{1}LLCT/^{1}MC	

Table S14 The Partial Molecular Orbital Compositions (%) by SCPA Approach in the Lowest-triplet State and Emission Transitions for Complex **1a** in the CH_2Cl_2 Solution Calculated by TD-DFT Method at the PBE1PBE Level.

orbital	energy (eV)	MO Contribution (%)			
		Pt (s/p/d)	Cu (s/p/d)	dpmp	C≡C$C_6H_3(CF_3)_2$-2,4
LUMO+1	-2.21	10.69 (19/0/81)	5.00 (48/43/9)	20.50	63.80
LUMO	-3.07	12.14 (0/100/0)	7.68 (29/53/18)	46.95	33.23
HOMO	-6.92	13.27 (8/0/91)	23.28 (14/9/78)	19.85	43.59
HOMO-2	-7.14	2.63 (2/81/16)	42.39 (27/5/68)	28.85	26.12

state	*E*, nm (eV)	O.S.	transition (contrib.)	assignment	measured (nm)
T_1	512 (2.42)	0.0000	HOMO→LUMO (69%)	^{3}IL/^{3}MC/^{3}MLCT/^{3}LLC	502
T_2	470 (2.64)	0.0000	HOMO-2→LUMO (51%) HOMO→LUMO+1 (23%)	^{3}IL/^{3}MLCT/^{3}MC ^{3}IL/^{3}MLCT/^{3}MC	

Table S15. The Partial Molecular Orbital Compositions (%) by SCPA Approach in the Ground State and Absorption Transitions for Complex **2a** in the CH_2Cl_2 Solution Calculated by TD-DFT Method at the PBE1PBE Level.

orbital	energy (eV)	MO Contribution (%)			
		Pt (s/p/d)	Cu (s/p/d)	dpmp	$C{\equiv}CC_6H_5$
LUMO+7	-1.43	26.13 (52/0/48)	10.23 (71/23/6)	58.67	4.97
LUMO+6	-1.46	4.11 (0/100/0)	7.91 (52/32/15)	84.75	3.24
LUMO+5	-1.50	3.27 (0/100/0)	6.54 (60/27/13)	78.99	11.21
LUMO+3	-1.55	7.51 (32/0/68)	3.88 (60/29/11)	74.57	14.04
LUMO+2	-1.61	11.31 (0/100/0)	6.44 (1/79/20)	80.26	1.99
LUMO+1	-1.75	18.77 (53/0/47)	2.25 (42/37/20)	75.21	3.76
LUMO	-2.67	15.92 (0/100/0)	8.33 (29/58/14)	57.03	18.73
HOMO	-6.56	16.32 (2/0/98)	16.54 (3/15/82)	11.60	55.54
HOMO-1	-6.86	0.83 (0/100/0)	35.01 (12/9/78)	26.60	37.56
HOMO-2	-7.06	25.41 (19/0/81)	41.12 (13/5/83)	29.98	3.49
HOMO-3	-7.26	13.81 (2/0/98)	21.72 (11/9/80)	32.76	31.71

state	*E*, nm (eV)	O.S.	transition (contrib.)	assignment	measured (nm)
S_1	409 (3.03)	0.2591	HOMO→LUMO (96%)	^{1}LLCT/^{1}IL/^{1}MC/^{1}MLCT	436
S_3	359 (3.45)	0.3748	HOMO-2→LUMO (90%)	^{1}MLCT/^{1}IL/^{1}MC	381
S_4	349 (3.55)	0.1687	HOMO-3→LUMO (88%)	^{1}IL/^{1}MC/^{1}LLCT/^{1}MLCT	
S_9	291 (4.26)	0.1648	HOMO→LUMO+2 (70%)	^{1}LLCT/^{1}MC/^{1}MLCT/^{1}IL	
			HOMO-1→LUMO+1 (11%)	^{1}LLCT/^{1}IL/^{1}MC/^{1}MLCT	
S_{10}	289 (4.29)	0.1056	HOMO-1→LUMO+1 (51%)	^{1}LLCT/^{1}IL/^{1}MC/^{1}MLCT	
			HOMO→LUMO+5 (24%)	^{1}LLCT/^{1}MLCT/^{1}IL/^{1}MC	
			HOMO→LUMO+6 (10%)	^{1}LLCT/^{1}MLCT/^{1}IL/^{1}MC	
S_{13}	283 (4.37)	0.2139	HOMO→LUMO+2 (18%)	^{1}LLCT/^{1}MC/^{1}MLCT/^{1}IL	
			HOMO→LUMO+5 (17%)	^{1}LLCT/^{1}MLCT/^{1}IL/^{1}MC	
			HOMO-1→LUMO+1 (15%)	^{1}LLCT/^{1}IL/^{1}MC/^{1}MLCT	
			HOMO-1→LUMO+3 (14%)	^{1}IL/^{1}MLCT/^{1}LLCT/^{1}MC	

Table S16. The Partial Molecular Orbital Compositions (%) by SCPA Approach in the Lowest-triplet State and Emission Transitions for Complex **2a** in the CH_2Cl_2 Solution Calculated by TD-DFT Method at the PBE1PBE Level.

orbital	energy (eV)	MO contribution (%)			
		Pt (s/p/d)	Cu (s/p/d)	dpmp	$C{\equiv}CC_6H_5$
LUMO	-2.91	14.55 (4/89/8)	7.60 (24/58/18)	53.62	24.23
HOMO	-6.33	12.96 (2/2/96)	20.76 (7/14/79)	16.46	49.83
HOMO-1	-6.78	3.97 (3/24/74)	31.30 (14/10/76)	23.38	41.35

state	*E*, nm (eV)	O.S.	transition (contrib.)	assignment	measured (nm)
T_1	594 (2.09)	0.0000	HOMO→LUMO (87%)	^{3}IL/^{3}LLCT/^{3}MC/^{3}MLCT	529
T_2	478 (2.59)	0.0000	HOMO-1→LUMO (75%)	^{3}IL/^{3}MC/^{3}LLCT/^{3}MLCT	

Table S17. The Partial Molecular Orbital Compositions (%) by SCPA Approach in the Ground State and Absorption Transitions for Complex **3a** in the CH_2Cl_2 Solution Calculated by TD-DFT Method at the PBE1PBE Level.

orbital	energy (eV)	MO Contribution (%)			
		Pt (s/p/d)	Cu (s/p/d)	dpmp	$C{\equiv}CC_6H_3(OMe)_2$-2,4
LUMO+6	-1.38	5.32 (0/100/0)	10.14 (77/18/5)	74.32	10.22
LUMO+5	-1.39	9.43 (0/100/0)	3.19 (32/21/47)	80.21	7.17
LUMO+3	-1.47	6.79 (0/100/0)	8.45 (47/40/12)	81.57	3.19
LUMO+1	-1.62	18.52 (34/0/66)	5.73 (43/50/7)	66.78	8.97
LUMO	-2.42	13.62 (0/100/0)	9.06 (28/61/11)	60.11	17.21
HOMO	-6.03	13.92 (3/0/97)	8.82 (4/18/78)	8.35	68.91
HOMO-1	-6.39	1.81 (0/100/0)	19.06 (20/14/66)	17.24	61.89
HOMO-2	-6.86	23.52 (21/0/79)	41.82 (13/5/82)	31.80	2.87
HOMO-3	-7.14	11.89 (2/0/98)	20.63 (11/12/77)	40.00	27.48

state	*E*, nm (eV)	O.S.	transition (contrib.)	assignment	measure (nm)
S_1	438 (2.83)	0.3925	HOMO→LUMO (97%)	^{1}LLCT/^{1}IL/^{1}MC	458
S_3	355 (3.50)	0.4038	HOMO-2→LUMO (94%)	^{1}MLCT/^{1}IL/^{1}MC	378
S_5	334 (3.71)	0.0927	HOMO-3→LUMO (89%)	^{1}IL/^{1}MC/^{1}LLCT/^{1}MLCT	
S_8	317 (3.91)	0.2969	HOMO→LUMO+3 (57%)	^{1}LLCT/^{1}MC/^{1}IL	
			HOMO→LUMO+6 (19%)	^{1}LLCT/^{1}IL/^{1}MC	
S_{10}	310 (4.00)	0.388	HOMO→LUMO+5 (49%)	^{1}LLCT/^{1}IL/^{1}MC/^{1}MLCT	
			HOMO-1→LUMO+1 (23%)	^{1}LLCT/^{1}IL/^{1}MC	

Table S18. The Partial Molecular Orbital Compositions (%) by SCPA Approach in the Lowest-triplet State and Emission Transitions for Complex **3a** in the CH_2Cl_2 Solution Calculated by TD-DFT Method at the PBE1PBE Level.

orbital	energy (eV)	MO contribution (%)			
		Pt (s/p/d)	Cu (s/p/d)	dpmp	$C{\equiv}CC_6H_3(OMe)_2$-2,4
LUMO	-2.68	15.39 (0/100/0)	8.69 (21/65/14)	58.41	17.51
HOMO	-5.83	14.06 (2/0/98)	7.43 (4/20/76)	7.01	71.50
HOMO-1	-6.28	2.53 (0/100/0)	19.01 (24/13/62)	16.79	61.67

state	*E*, nm (eV)	O.S.	transition (contrib.)	assignment	measured (nm)
T_1	613 (2.02)	0.0000	HOMO→LUMO (90%)	^{3}LLCT/^{3}IL/^{3}MC	572
T_2	499 (2.48)	0.0000	HOMO-1→LUMO (77%)	^{3}LLCT/^{3}IL/^{3}MC	

Table S19. The Partial Molecular Orbital Compositions (%) by SCPA Approach in the Ground State and Absorption Transitions for Complex **4a** in the CH_2Cl_2 Solution Calculated by TD-DFT Method at the PBE1PBE Level.

orbital	energy (eV)	MO contribution (%)			
		Pt (s/p/d)	Cu (s/p/d)	dpmp	C≡C$C_6H_4NMe_2$-4
LUMO+23	-0.47	7.70 (0/100/0)	13.60 (75/19/5)	53.29	25.40
LUMO+13	-0.87	36.41 (87/0/13)	25.27 (82/17/1)	36.44	1.88
LUMO+8	-1.15	2.10 (0/100/0)	3.41 (49/42/9)	82.21	12.27
LUMO+6	-1.35	5.05 (0/100/0)	7.68 (59/33/8)	83.25	4.03
LUMO+5	-1.39	6.28 (26/0/74)	5.98 (29/60/12)	82.82	4.92
LUMO+4	-1.41	3.97 (0/100/0)	3.86 (44/18/38)	90.03	2.14
LUMO+2	-1.54	11.75 (0/100/0)	6.66 (5/77/19)	79.80	1.79
LUMO+1	-1.65	16.06 (52/0/48)	1.98 (34/36/30)	79.15	2.82
LUMO	-2.44	14.77 (0/100/0)	7.87 (21/67/13)	62.03	15.33
HOMO	-5.56	8.10 (2/0/98)	5.38 (13/25/62)	3.91	82.61
HOMO-1	-5.83	1.65 (0/100/0)	7.45 (24/20/56)	7.35	83.56
HOMO-2	-6.90	19.28 (23/0/77)	40.08 (14/6/80)	32.78	7.85
HOMO-3	-6.98	15.53 (3/0/97)	22.36 (6/8/86)	26.82	35.29

state	*E*, nm (eV)	O.S.	transition (contrib.)	assignment	measured (nm)
S_1	499 (2.49)	0.5905	HOMO→LUMO (97%)	^{1}LLCT/^{1}IL/^{1}MC	500
S_5	352 (3.52)	0.3752	HOMO-2→LUMO (71%)	^{1}IL/^{1}MLCT/^{1}MC	378
			HOMO-3→LUMO (19%)	^{1}IL/^{1}MC/^{1}LLCT	
S_{13}	334 (3.71)	0.2369	HOMO→LUMO+6 (42%)	^{1}LLCT/^{1}MC	
			HOMO-1→LUMO+1 (26%)	^{1}LLCT/^{1}IL/^{1}LMCT	
			HOMO→LUMO+4 (20%)	^{1}LLCT	
S_{16}	322 (3.85)	0.4126	HOMO→LUMO+8 (67%)	^{1}LLCT/^{1}IL	
			HOMO-1→LUMO+5 (12%)	^{1}LLCT/^{1}IL	
S_{53}	271 (4.58)	0.1875	HOMO→LUMO+23 (30%)	^{1}LLCT/^{1}IL/^{1}MC	
			HOMO-2→LUMO+2 (15%)	^{1}MLCT/^{1}IL/^{1}MC	
			HOMO-1→LUMO+13 (11%)	^{1}LMCT/^{1}LLCT	

Table S20 The Partial Molecular Orbital Compositions (%) by SCPA Approach in the Lowest-triplet State and Emission Transitions for Complex **4a** in the CH_2Cl_2 Solution Calculated by TD-DFT Method at the PBE1PBE Level.

orbital	energy (eV)	MO contribution (%)			
		Pt (s/p/d)	Cu (s/p/d)	dpmp	C≡C$C_6H_4NMe_2$-4
LUMO	-2.67	14.29 (0/100/0)	7.95 (22/62/16)	61.33	16.43
HOMO	-5.46	9.06 (1/0/99)	4.75 (7/28/65)	4.04	82.15
HOMO-1	-5.80	1.21 (0/100/0)	6.51 (4/26/70)	8.97	83.31

state	*E*, nm (eV)	O.S.	transition (contrib.)	assignment	measured (nm)
T_1	674 (1.84)	0.0000	HOMO→LUMO (91%)	^{3}LLCT/^{3}IL/^{3}MC	653
T_2	554 (2.24)	0.0000	HOMO-1→LUMO (86%)	^{3}LLCT/^{3}IL/^{3}LMCT	

Table S21. The Partial Molecular Orbital Compositions (%) by SCPA Approach in the Ground State and Absorption Transitions for Complex **1b** in the CH_2Cl_2 Solution Calculated by TD-DFT Method at the PBE1PBE Level.

orbital	energy (eV)	MO contribution (%)			
		Pt (s/p/d)	Cu (s/p/d)	dTolmp	$C{\equiv}CC_6H_3(CF_3)_2$-2,4
LUMO+10	-1.28	1.58 (0/100/0)	10.96 (74/15/10)	81.97	5.48
LUMO+7	-1.38	8.13 (0/100/0)	8.32 (5/75/20)	76.32	7.23
LUMO+3	-1.68	20.69 (58/0/42)	3.58 (60/34/6)	71.07	4.65
LUMO+1	-2.25	2.67 (0/100/0)	3.48 (55/28/17)	19.68	74.16
LUMO	-2.69	13.04 (0/100/0)	12.38 (49/36/15)	62.20	12.38
HOMO	-6.91	12.30 (25/0/75)	39.70 (26/4/70)	38.57	9.42
HOMO-2	-7.12	15.25 (5/0/95)	14.65 (7/14/79)	27.81	42.29
HOMO-3	-7.28	0.94 (0/100/0)	16.71 (8/24/68)	53.49	28.85
HOMO-4	-7.41	6.74 (2/0/98)	6.62 (2/53/45)	75.41	11.23
HOMO-6	-7.49	16.47 (3/0/97)	18.44 (1/3/96)	45.89	19.21
HOMO-7	-7.55	15.95 (4/0/96)	14.79 (5/4/90)	47.70	21.56
HOMO-31	-8.68	11.76 (10/0/90)	77.57 (2/0/98)	8.35	2.32

state	*E*, nm (eV)	O.S.	transition (contrib.)	assignment	measured (nm)
S_1	379 (3.27)	0.1996	HOMO→LUMO (96%)	^{1}IL/^{1}MLCT/^{1}MC	385
S_3	357 (3.47)	0.1145	HOMO-2→LUMO (94%)	^{1}IL/^{1}LLCT/^{1}MC	
S_5	327 (3.79)	0.2301	HOMO-6→LUMO (53%)	^{1}IL/^{1}MC/^{1}MLCT	
			HOMO-7→LUMO (35%)	^{1}IL/^{1}MC/^{1}LLCT	
S_{10}	297 (4.17)	0.4476	HOMO-2→LUMO+1 (79%)	^{1}IL/^{1}MLCT	
S_{31}	272 (4.56)	0.125	HOMO-4→LUMO+1 (67%)	^{1}LLCT/^{1}IL	
S_{60}	256 (4.84)	0.1399	HOMO-31→LUMO (24%)	^{1}MLCT/^{1}MC	
			HOMO→LUMO+7 (14%)	^{1}IL/^{1}MLCT/^{1}MC	
			HOMO-3→LUMO+3 (12%)	^{1}IL/^{1}LLCT/^{1}MC	

Table S22. The Partial Molecular Orbital Compositions (%) by SCPA Approach in the Lowest-triplet State and Emission Transitions for Complex **1b** in the CH_2Cl_2 Solution Calculated by TD-DFT Method at the PBE1PBE Level.

orbital	energy (eV)	MO contribution (%)			
		Pt (s/p/d)	Cu (s/p/d)	dTolmp	$C{\equiv}CC_6H_3(CF_3)_2$-2,4
LUMO+1	-2.29	2.72	2.93	24.85	69.50
LUMO	-3.08	14.00	10.49	51.75	23.76
HOMO	-6.42	5.40	37.35	39.70	17.55
HOMO-1	-6.94	8.46	18.88	39.79	32.87

state	*E*, nm (eV)	O.S.	transition (contrib.)	assignment	measured (nm)
T_1	597 (2.08)	0.0000	HOMO→LUMO (89%)	^{3}IL/^{3}MC	538
T_2	491 (2.52)	0.0000	HOMO-1→LUMO (51%)	^{3}IL/^{3}MC/^{3}LLCT	
			HOMO→LUMO+1 (10%)	^{3}IL/^{3}MLCT/^{3}LLCT	

Table S23. The Partial Molecular Orbital Compositions (%) by SCPA Approachin the Ground State and Absorption Transitions for Complex **2b** in the CH_2Cl_2 Solution Calculated by TD-DFT Method at the PBE1PBE Level.

orbital	energy (eV)	MO contribution (%)			
		Pt (s/p/d)	Cu (s/p/d)	dTolmp	C≡CC_6H_5
LUMO+8	-1.27	8.08 (13/74/13)	7.49 (31/61/8)	60.98	23.45
LUMO+5	-1.43	6.53 (40/28/33)	12.21 (61/30/9)	77.53	3.73
LUMO+1	-1.70	27.24 (45/35/20)	9.12 (73/23/4)	49.79	13.86
LUMO	-2.67	19.85 (12/76/12)	11.28 (48/41/11)	56.71	12.16
HOMO	-6.57	11.06 (12/1/87)	24.73 (17/9/74)	20.48	43.72
HOMO-1	-6.74	8.52 (11/10/79)	29.02 (11/8/80)	25.21	37.25
HOMO-2	-6.96	18.23 (16/2/82)	35.29 (20/4/75)	33.00	13.48
HOMO-16	-7.81	2.90 (14/63/23)	4.85 (64/29/6)	9.86	82.39

state	*E*, nm (eV)	O.S.	transition (Contrib.)	assignment	measured (nm)
S_1	414 (2.99)	0.0560	HOMO→LUMO (96%)	^{1}LLCT/^{1}IL/^{1}MC	435
S_2	391 (3.17)	0.1672	HOMO-1→LUMO (95%)	^{1}IL/^{1}MC/^{1}LLCT	390
S_3	370 (3.36)	0.2558	HOMO-2→LUMO (93%)	^{1}IL/^{1}MC/^{1}MLCT	
S_7	306 (4.05)	0.1409	HOMO→LUMO+1 (77%)	^{1}MC/^{1}IL/^{1}LLCT	
S_9	293 (4.23)	0.1135	HOMO-1→LUMO+1 (62%)	^{1}IL/^{1}MC/^{1}LLCT	
			HOMO-2→LUMO+1 (9%)	^{1}IL/^{1}MC/^{1}MLCT	
S_{27}	276 (4.49)	0.1181	HOMO→LUMO+8 (23%)	^{1}IL/^{1}LLCT/^{1}MLCT/^{1}MC	
			HOMO→LUMO+5 (11%)	^{1}LLCT/^{1}IL/^{1}MC/^{1}MLCT	
			HOMO-16→LUMO (10%)	^{1}LLCT/^{1}LMCT/^{1}IL	

Table S24. The Partial Molecular Orbital Compositions (%) by SCPA Approach in the Lowest-triplet State and Emission Transitions for Complex **2b** in the CH_2Cl_2 Solution Calculated by TD-DFT Method at the PBE1PBE Level.

orbital	energy (eV)	MO contribution (%)			
		Pt (s/p/d)	Cu (s/p/d)	dTolmp	C≡CC_6H_5
LUMO	-3.20	23.00 (28/33/39)	7.37 (42/38/21)	50.23	19.39
HOMO	-6.32	11.99 (8/5/86)	24.72 (7/12/81)	23.09	40.19
HOMO-1	-6.66	5.58 (27/6/68)	30.38 (18/9/73)	26.53	37.50

state	*E*, nm (eV)	O.S.	transition (contrib.)	assignment	measured (nm)
T_1	603 (2.06)	0.0000	HOMO→LUMO (91%)	^{3}IL/^{3}MC/^{3}LLCT	545
T_2	528 (2.35)	0.0000	HOMO-1→LUMO (84%)	^{3}IL/^{3}MC/^{3}LLCT	

Table S25. The Partial Molecular Orbital Compositions (%) by SCPA Approach in the Ground State and Absorption Transitions for Complex **3b** in the CH_2Cl_2 Solution Calculated by TD-DFT Method at the PBE1PBE Level.

orbital	energy (eV)	MO Contribution (%)			
		Pt (s/p/d)	Cu (s/p/d)	dTolmp	C≡C$C_6H_3(OMe)_2$-2,4
LUMO+10	-1.02	25.18 (75/9/16)	13.53 (84/14/2)	51.59	9.70
LUMO+9	-1.03	16.18 (52/26/22)	15.34 (84/13/3)	45.11	23.38
LUMO+3	-1.43	18.79 (70/5/26)	4.86 (47/44/9)	73.66	2.69
LUMO+1	-1.54	11.78 (45/20/34)	1.54 (14/46/40)	81.34	5.33
LUMO	-2.53	19.54 (21/61/18)	8.20 (33/52/15)	58.97	13.29
HOMO	-6.14	8.85 (3/7/90)	7.99 (5/18/77)	8.99	74.17
HOMO-1	-6.20	8.48 (7/11/82)	9.64 (8/15/78)	11.43	70.46
HOMO-2	-6.71	11.84 (24/2/74)	40.37 (20/5/75)	35.21	12.58
HOMO-3	-7.03	13.98 (15/3/82)	42.26 (18/4/78)	30.91	12.85

state	*E*, nm (eV)	O.S.	transition (contrib.)	assignment	measured (nm)
S_1	440 (2.82)	0.0848	HOMO→LUMO (94%)	^{1}LLCT/^{1}IL/^{1}MC/^{1}LMCT	450
S_2	428 (2.90)	0.2389	HOMO-1→LUMO (93%)	^{1}LLCT/^{1}IL/^{1}MC/^{1}LMCT	
S_3	382 (3.24)	0.1495	HOMO-2→LUMO (96%)	^{1}IL/^{1}MC/^{1}MLCT	388
S_4	350 (3.54)	0.1751	HOMO-3→LUMO (89%)	^{1}IL/^{1}MLCT/^{1}MC	
S_6	317 (3.91)	0.1472	HOMO→LUMO+1 (39%)	^{1}LLCT/^{1}IL/^{1}MC	
			HOMO→LUMO+3 (15%)	^{1}LLCT/^{1}MC	
S_{29}	282 (4.40)	0.2012	HOMO→LUMO+9 (32%)	^{1}LLCT/^{1}IL/^{1}MC/^{1}LMCT	
			HOMO→LUMO+10 (24%)	^{1}LLCT/^{1}LMCT/^{1}IL/^{1}MC	

Table S26. The Partial Molecular Orbital Compositions (%) by SCPA Approach in the Lowest-triplet State and Emission Transitions for Complex **3b** in the CH_2Cl_2 Solution Calculated by TD-DFT Method at the PBE1PBE Level.

orbital	energy (eV)	MO contribution (%)			
		Pt (s/p/d)	Cu (s/p/d)	dTolmp	C≡C$C_6H_3(OMe)_2$-2,4
LUMO	-2.96	23.37 (33/31/36)	7.48 (46/38/17)	51.16	17.98
HOMO	-5.95	11.99 (9/10/81)	15.48 (5/20/75)	14.91	57.61
HOMO-1	-6.14	5.21 (19/7/74)	8.48 (15/13/72)	12.37	73.93

state	*E*, nm (eV)	O.S.	transition (contrib.)	assignment	measured (nm)
T_1	650 (1.91)	0.0000	HOMO→LUMO (90%)	^{3}LLCT/^{3}IL/^{3}MC	593
T_2	541 (2.29)	0.0000	HOMO-1→LUMO (91%)	^{3}LLCT/^{3}IL/^{3}LMCT/^{3}MC	

Table S27. The Partial Molecular Orbital Compositions (%) by SCPA Approach in the Ground State and Absorption Transitions for Complex **4b** in the CH_2Cl_2 Solution Calculated by TD-DFT Method at the PBE1PBE Level.

orbital	energy (eV)	MO Contribution (%)			
		Pt (s/p/d)	Cu (s/p/d)	dTolmp	$C{\equiv}CC_6H_4NMe_2$-4
LUMO+7	-1.23	43.89 (75/6/19)	15.19 (77/20/2)	36.63	4.29
LUMO+6	-1.26	10.27 (38/58/4)	8.90 (50/38/12)	78.76	2.08
LUMO+1	-1.60	23.89 (38/38/24)	8.82 (80/16/4)	55.17	12.12
LUMO	-2.51	20.42 (23/60/17)	8.06 (34/53/14)	60.53	10.99
HOMO	-5.58	7.78 (0/15/85)	7.58 (31/19/50)	4.99	79.64
HOMO-1	-5.79	2.61 (5/55/40)	7.97 (21/17/62)	8.68	80.74
HOMO-2	-6.77	14.14 (22/3/75)	40.42 (24/5/72)	34.83	10.60

state	*E*, nm (eV)	O.S.	transition (Contrib.)	assignment	measured (nm)
S_1	517 (2.40)	0.3141	HOMO→LUMO (96%)	^{1}LLCT/^{1}MC/^{1}LMCT/^{1}IL	492
S_2	469 (2.64)	0.0742	HOMO-1→LUMO (95%)	^{1}LLCT/^{1}IL/^{1}LMCT	
S_3	372 (3.33)	0.3587	HOMO-2→LUMO (82%)	^{1}IL/^{1}MC/^{1}MLCT	380
S_8	342 (3.63)	0.082	HOMO-1→LUMO+1 (69%)	^{1}LLCT/^{1}LMCT/^{1}IL	
S_{22}	310 (4.00)	0.1442	HOMO-1→LUMO+6 (58%)	^{1}LLCT	
			HOMO-1→LUMO+7 (13%)	^{1}LMCT/^{1}LLCT	

Table S28. The Partial Molecular Orbital Compositions (%) by SCPA Approach in the Lowest-triplet State and Emission Transitions for Complex **4b** in the CH_2Cl_2 Solution Calculated by TD-DFT Method at the PBE1PBE Level.

orbital	energy (eV)	MO contribution (%)			
		Pt (s/p/d)	Cu (s/p/d)	dTolmp	$C{\equiv}CC_6H_4NMe_2$-4
LUMO	-2.95	24.98 (35/36/29)	6.93 (41/42/17)	52.66	15.42
HOMO	-5.50	8.03 (4/3/93)	5.78 (10/21/69)	5.13	81.06
HOMO-1	-5.76	3.69 (33/39/28)	8.51 (23/19/58)	11.02	76.78

state	*E*, nm (eV)	O.S.	transition (contrib.)	assignment	measured (nm)
T_1	723 (1.71)	0.0000	HOMO→LUMO (89%)	^{3}LLCT/^{3}IL/^{3}LMCT/^{3}MC	672
T_2	635 (1.95)	0.0000	HOMO-1→LUMO (89%)	^{3}LLCT/^{3}IL/^{3}LMCT/^{3}MC	

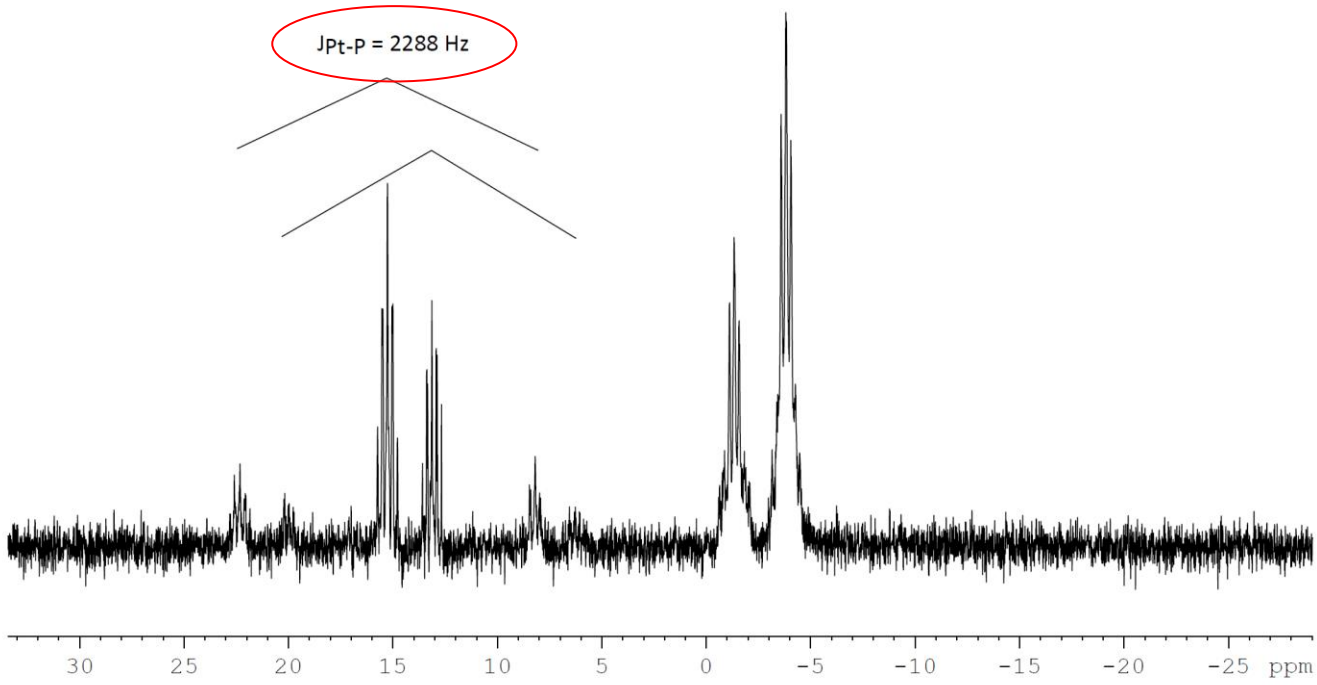

Fig. S1 The ^{31}P NMR spectrum of dpmp-supported $PtCu_2$ complex **1a**, measured in CD_2Cl_2.

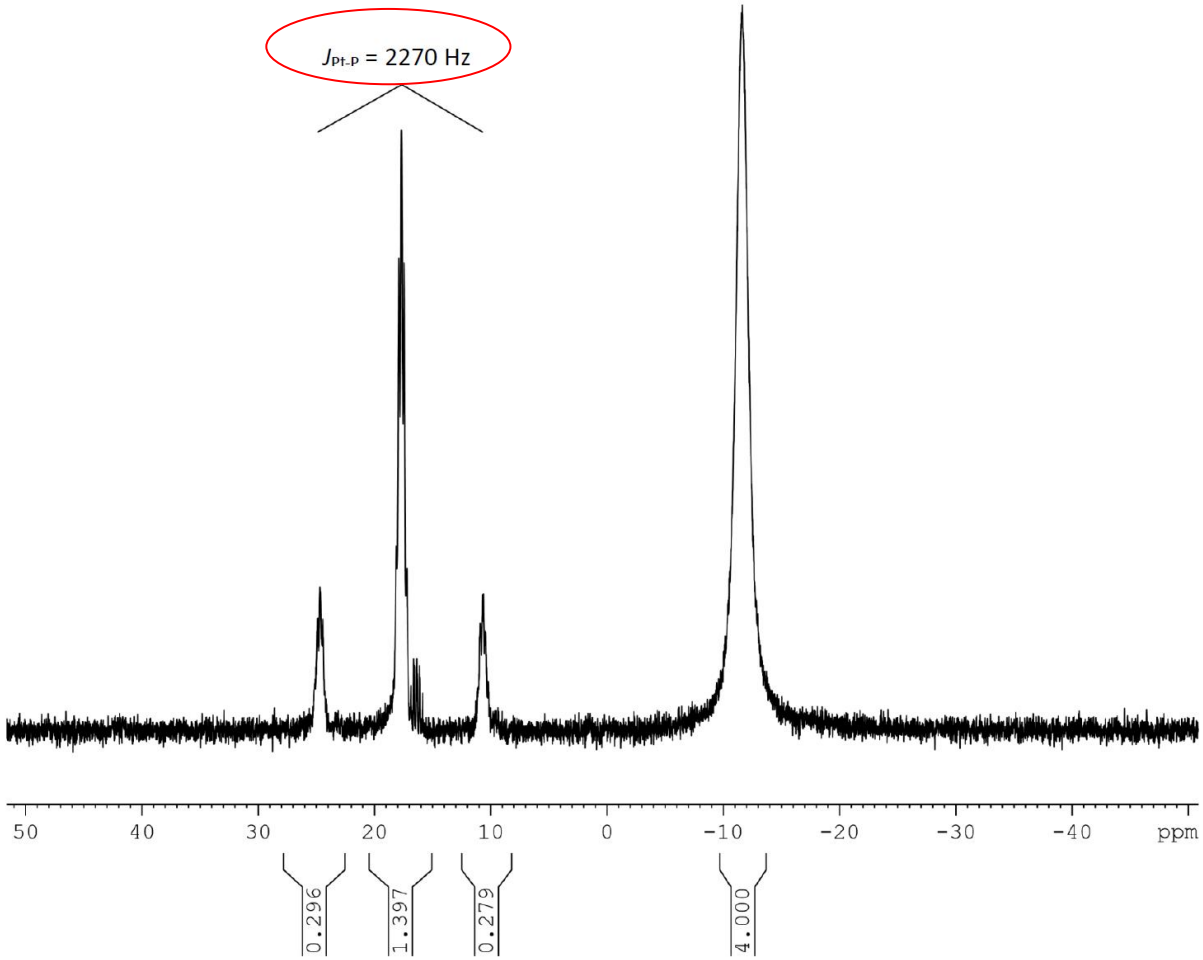

Fig. S2 The ^{31}P NMR spectrum of dTolmp-supported $PtCu_2$ complex **1b**, measured in CD_2Cl_2.

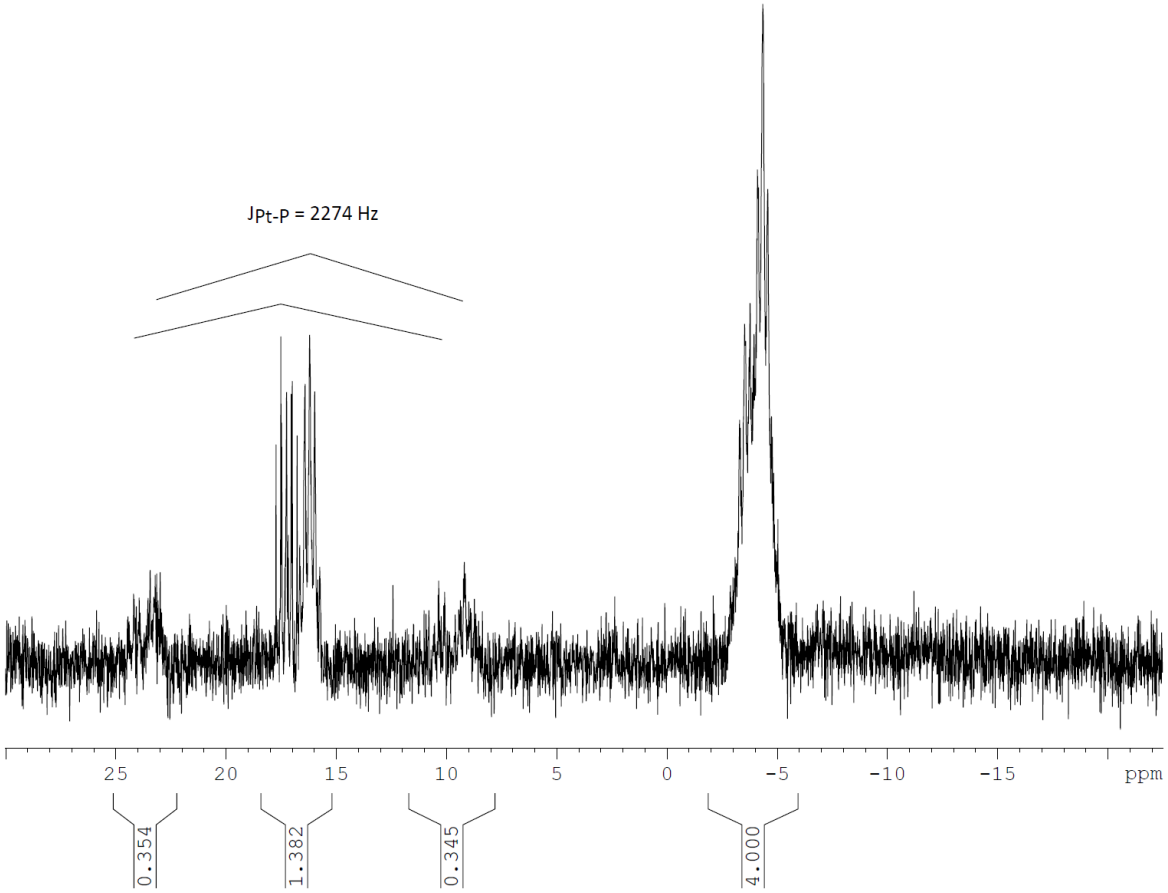

Fig. S3 The ^{31}P NMR spectrum of dpmp-supported $PtCu_2$ complex **2a**, measured in CD_2Cl_2.

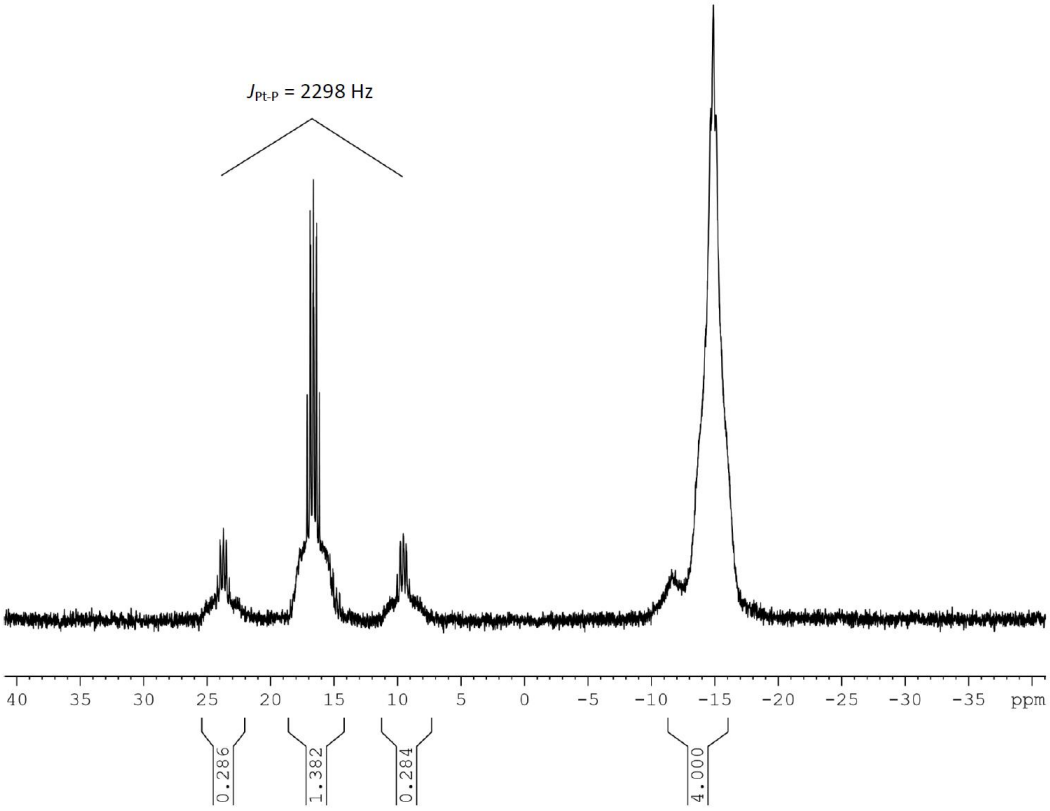

Fig. S4 The ^{31}P NMR spectrum of dTolmp-supported $PtCu_2$ complex **2b**, measured in CD_2Cl_2.

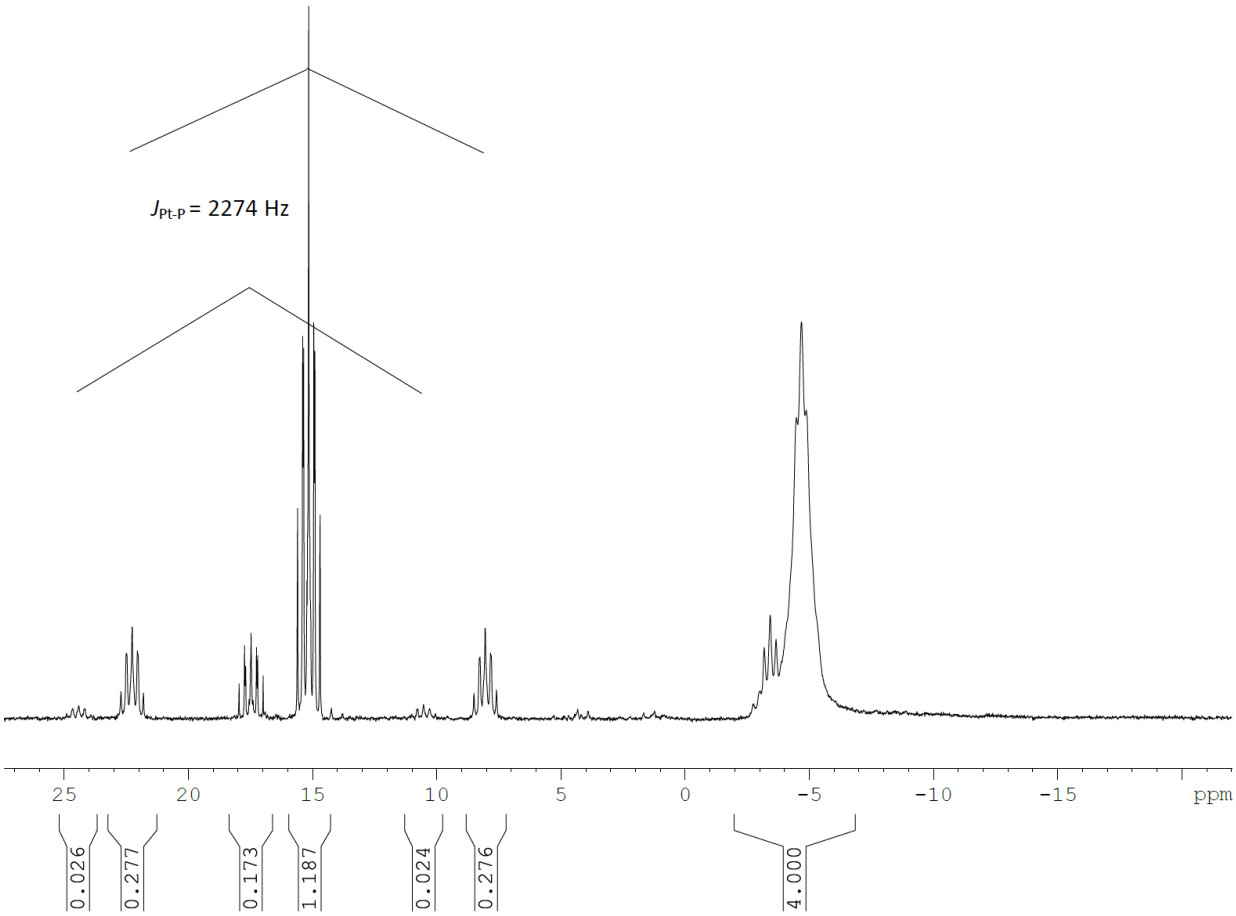

Fig. S5 The ^{31}P NMR spectrum of dpmp-supported $PtCu_2$ complex **3a**, measured in CD_2Cl_2.

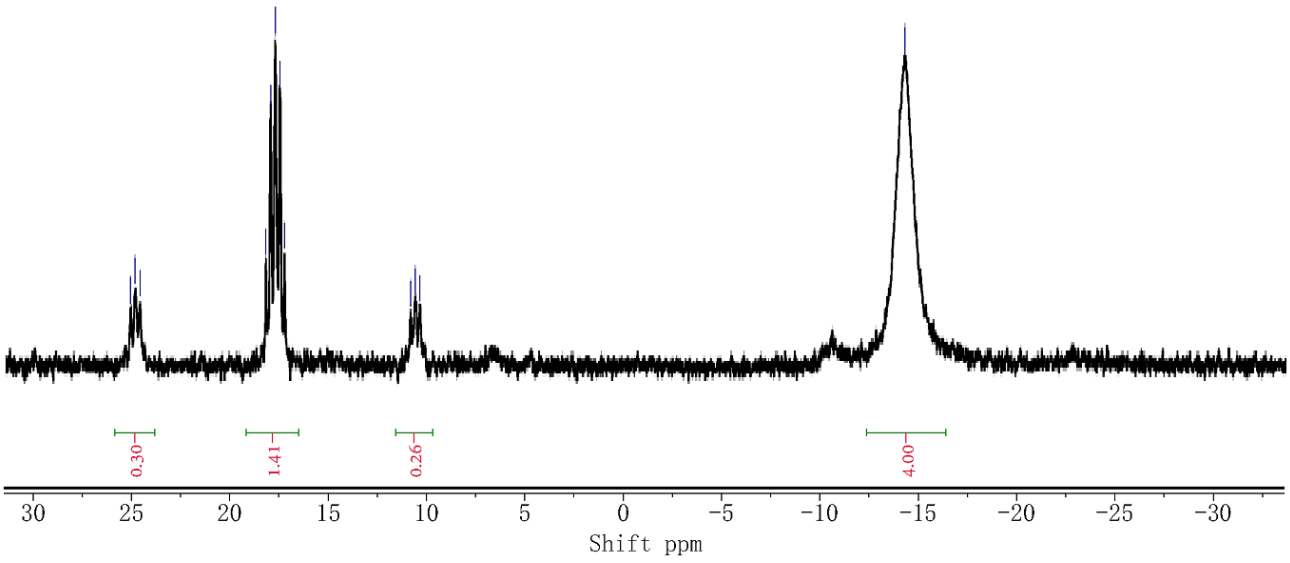

Fig. S6 The ^{31}P NMR spectrum of dTolmp-supported $PtCu_2$ complex **3b**, measured in CD_2Cl_2.

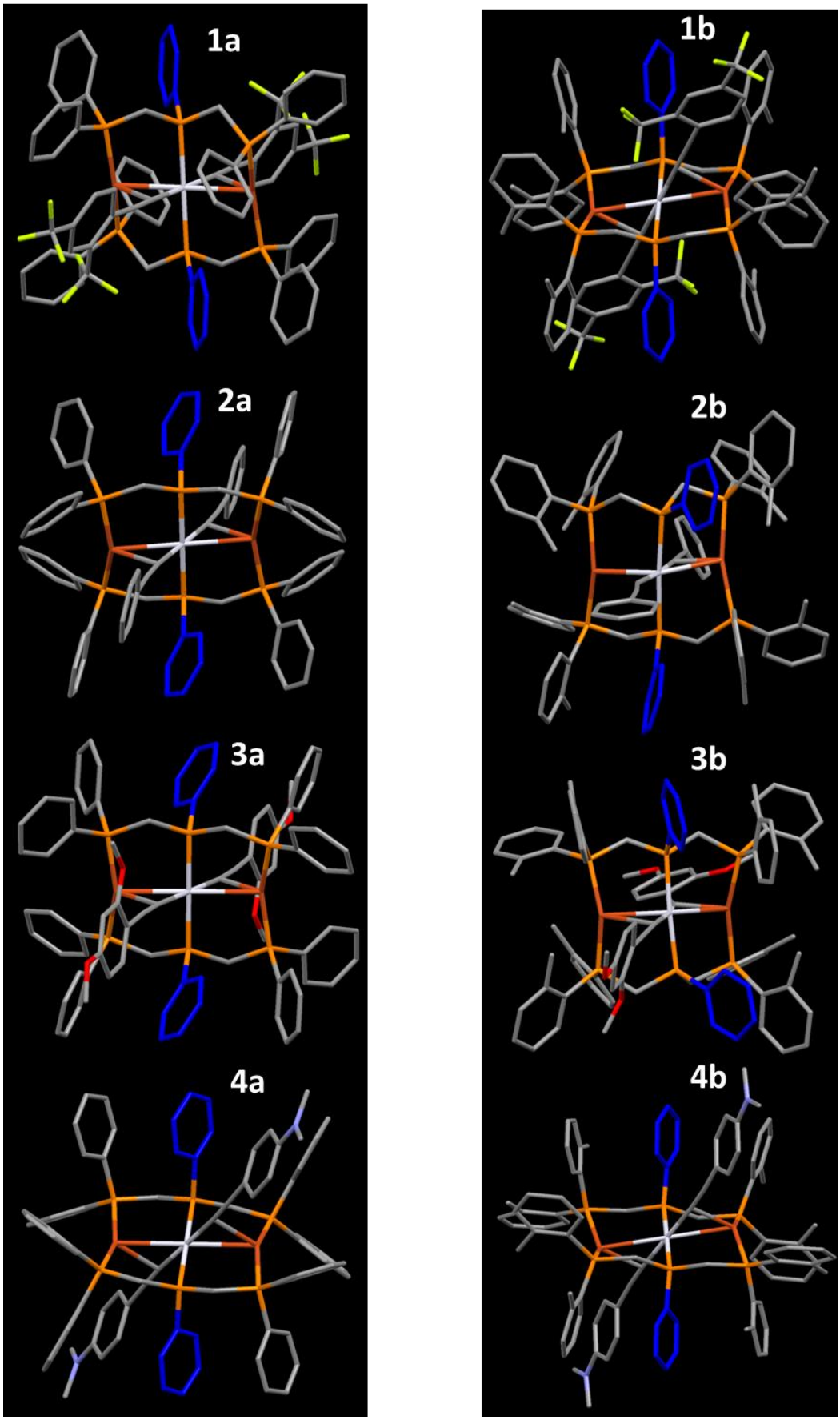

Fig. S7 Perspective views of dpmp-supported $PtCu_2$ complexes **1a**–**4a** and dTolmp-supported $PtCu_2$ complexes **1b**–**4b**.

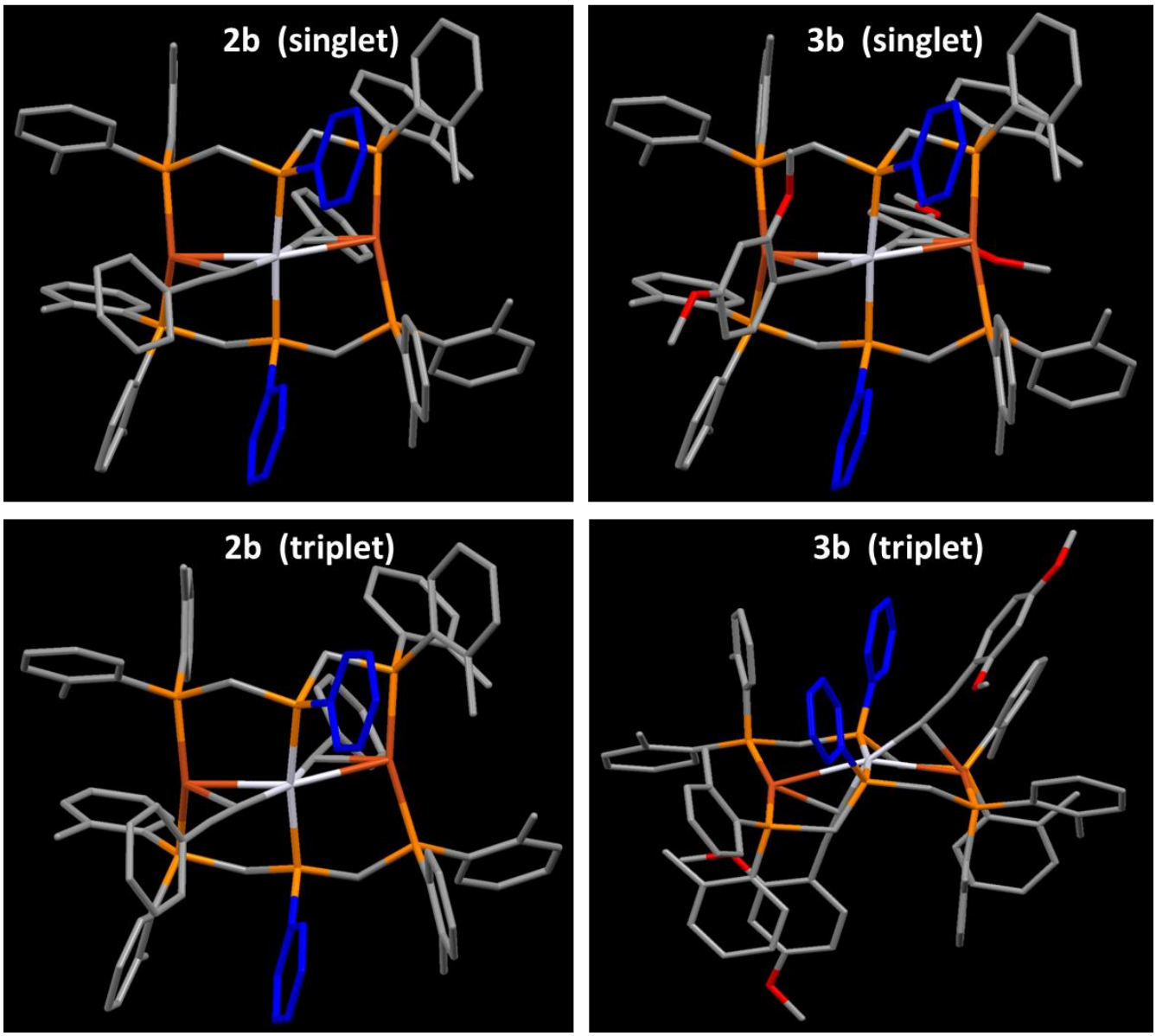

Fig. S8 The optimized structures of complexes **2b** and **3b** in the ground and triplet states by DFT method, showing that the phenyl rings at the middle P donors of the two dTolmp ligands are *syn*-arranged.

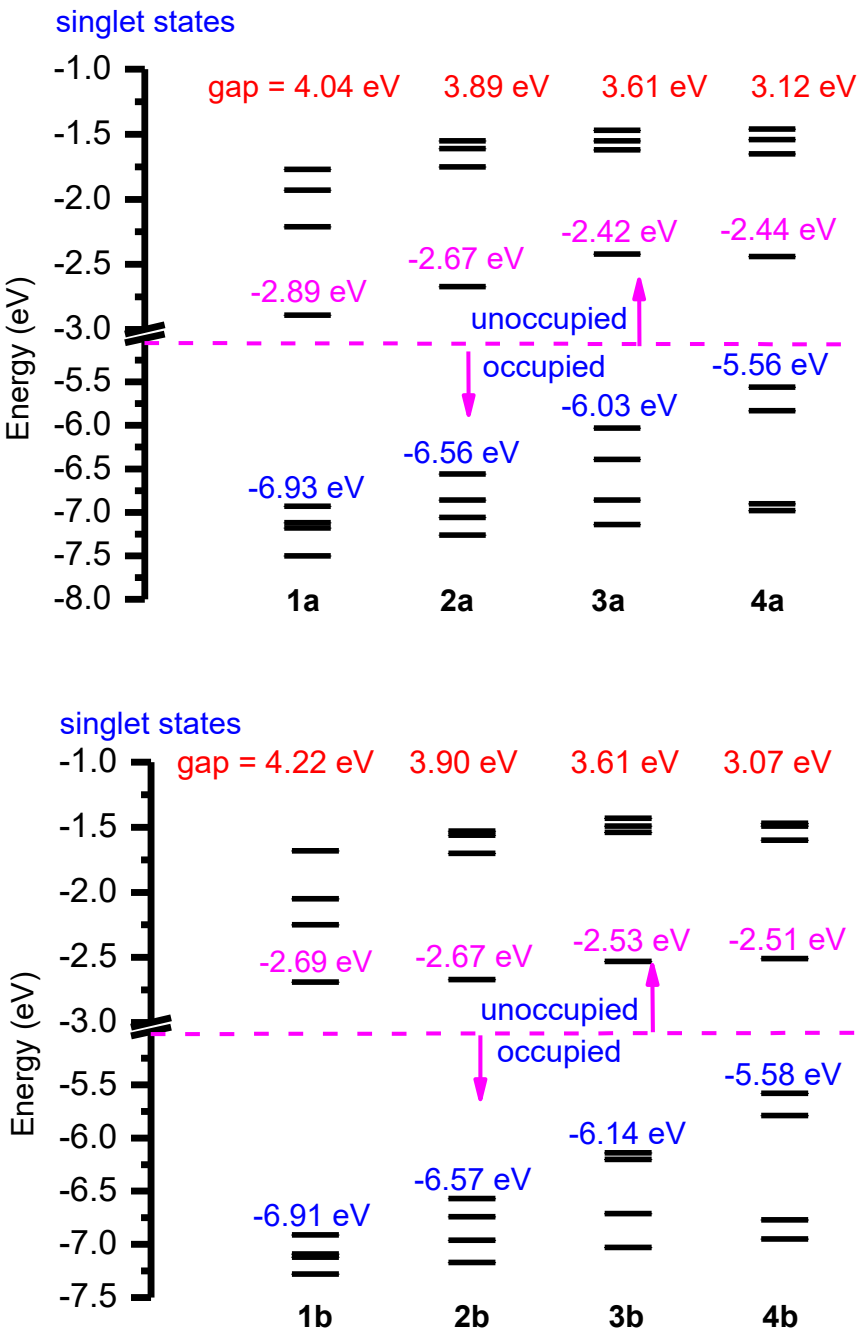

Fig. S9 The plots of energy level of frontier orbitals in the ground states for complexes **1a**–**4a** and **1b**–**4b** in the CH_2Cl_2 by TD-DFT method at the PBE1PBE level.

	LUMO	HOMO
S_1	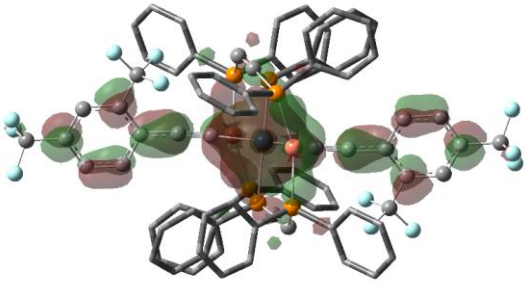	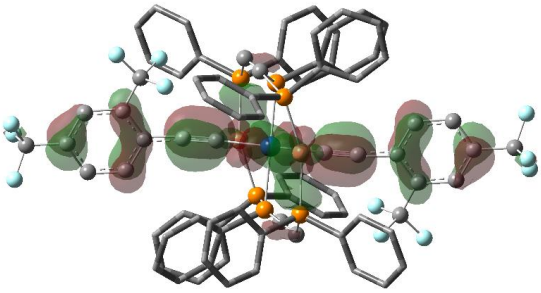
T_1	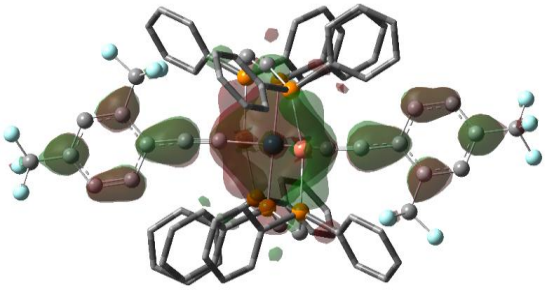	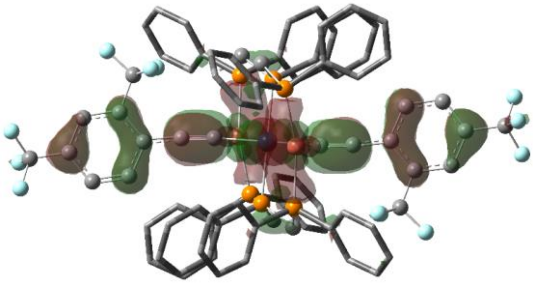

Fig. S10 The plots of HOMO and LUMO involved in the absorption (S_0) and emission (T_1) transitions for complex **1a** in the CH_2Cl_2 calculated by TD-DFT method at the PBE1PBE level (isovalue = 0.02).

	LUMO	HOMO
S_1	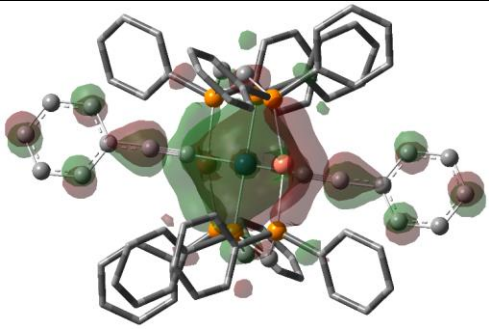	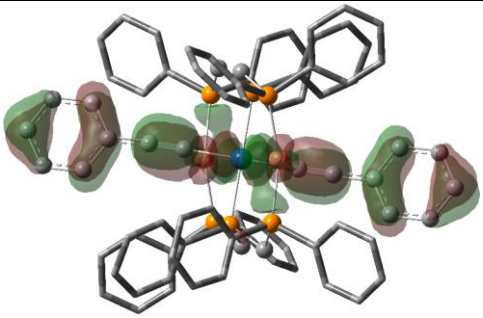
T_1	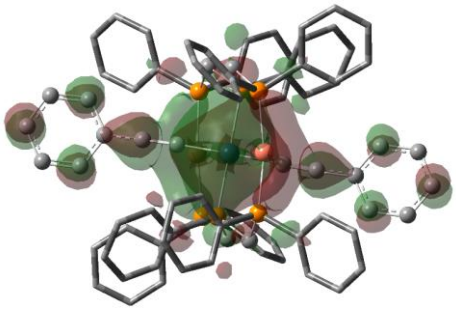	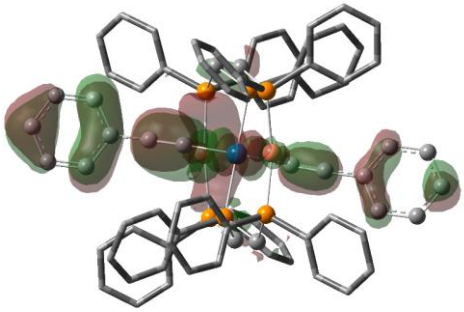

Fig. S11 The plots of HOMO and LUMO involved in the absorption (S_0) and emission (T_1) transitions for complex **2a** in the CH_2Cl_2 calculated by TD-DFT method at the PBE1PBE level (isovalue = 0.02).

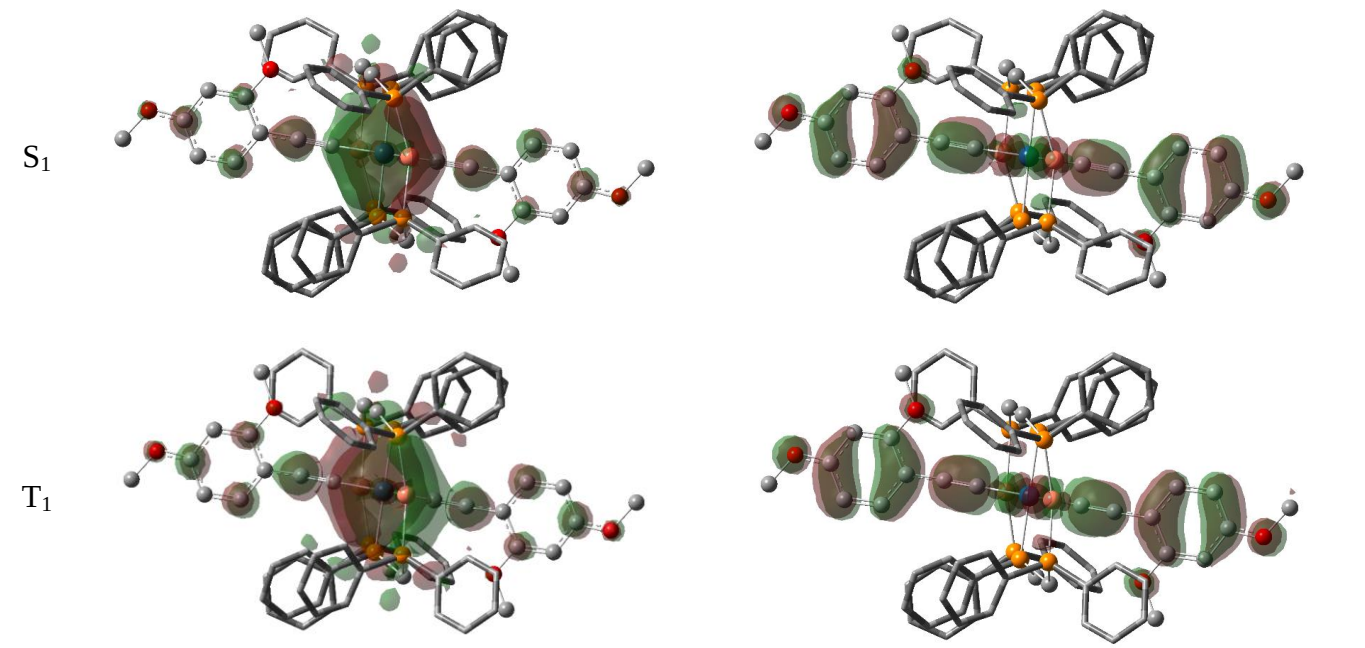

Fig. S12 The plots of HOMO and LUMO involved in the absorption (S_0) and emission (T_1) transitions for complex **3a** in the CH_2Cl_2 calculated by TD-DFT method at the PBE1PBE level (isovalue = 0.02).

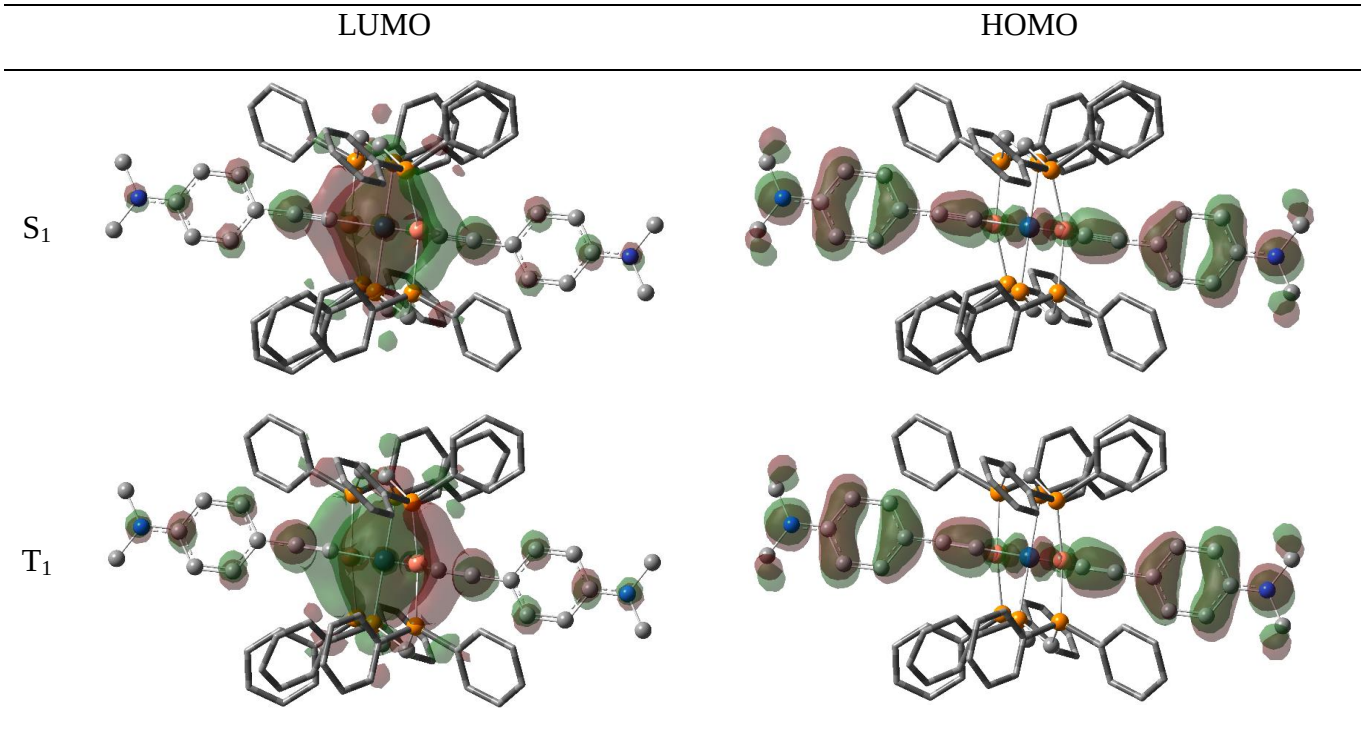

Fig. S13 The plots of HOMO and LUMO involved in the absorption (S_0) and emission (T_1) transitions for complex **4a** in the CH_2Cl_2 calculated by TD-DFT method at the PBE1PBE level (isovalue = 0.02).

	LUMO	HOMO
S_1	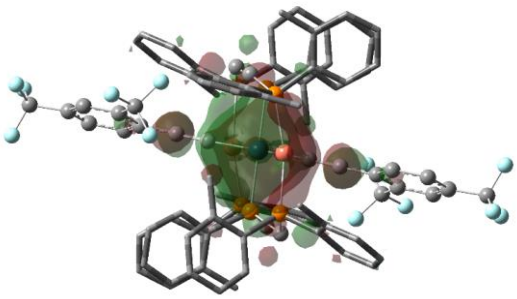	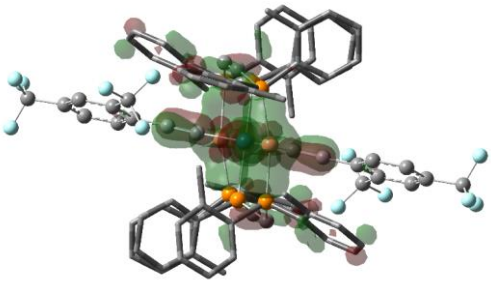
T_1		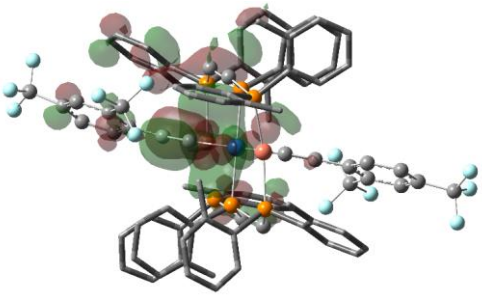

Fig. S14 The plots of HOMO and LUMO involved in the absorption (S_0) and emission (T_1) transitions for complex **1b** in the CH_2Cl_2 calculated by TD-DFT method at the PBE1PBE level (isovalue = 0.02).

	LUMO	HOMO
S_1	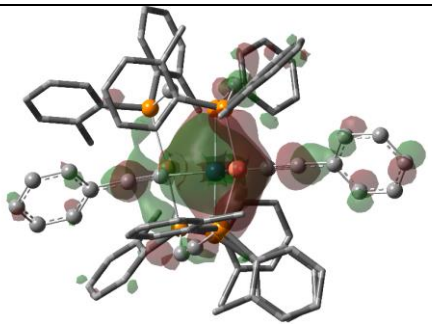	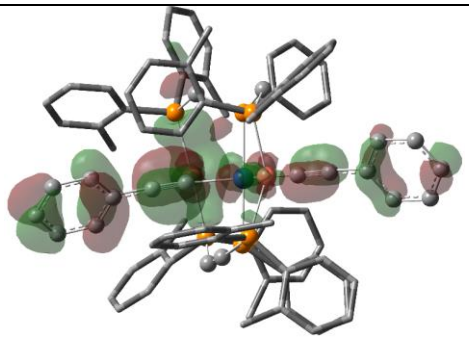
T_1	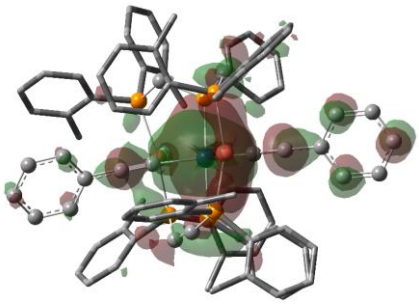	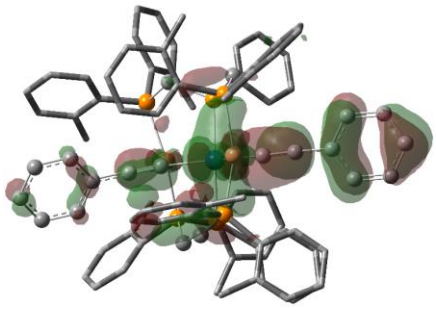

Fig. S15 The plots of HOMO and LUMO involved in the absorption (S_0) and emission (T_1) transitions for complex **2b** in the CH_2Cl_2 calculated by TD-DFT method at the PBE1PBE level (isovalue = 0.02).

	LUMO	HOMO
S_1	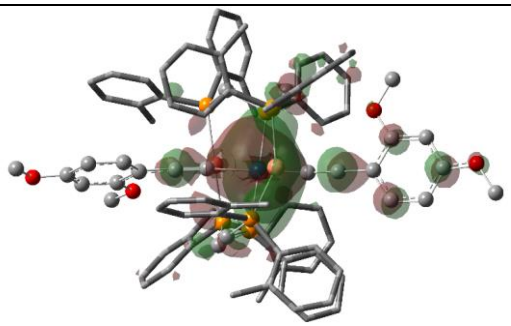	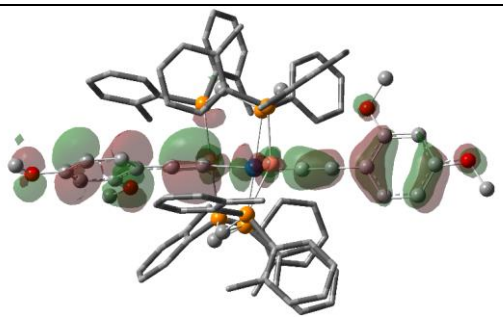
T_1	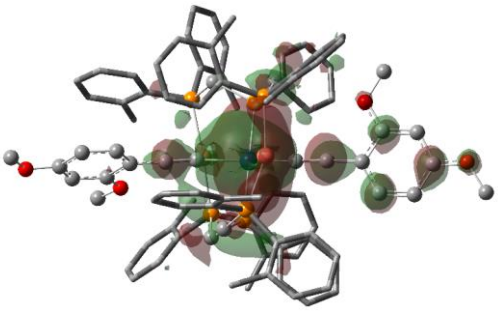	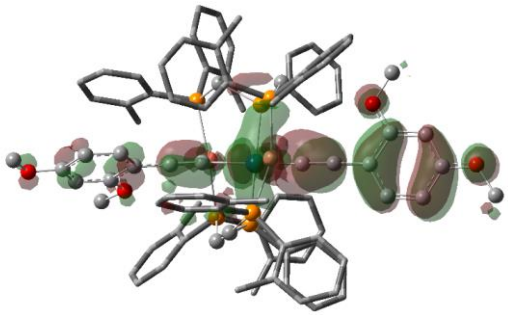

Fig. S16 The plots of HOMO and LUMO involved in the absorption (S_0) and emission (T_1) transitions for complex **3b** in the CH_2Cl_2 calculated by TD-DFT method at the PBE1PBE level (isovalue = 0.02).

	LUMO	HOMO
S_1	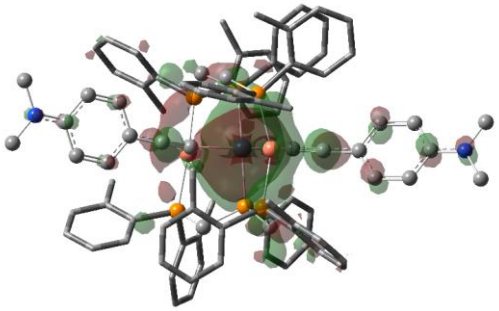	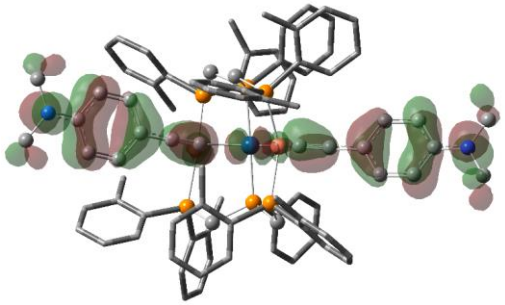
T_1	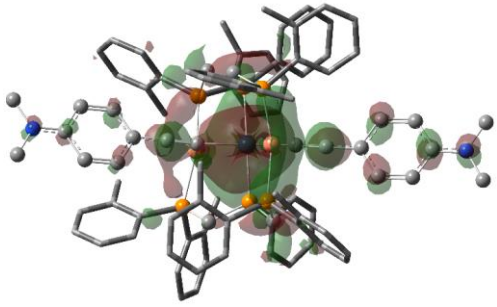	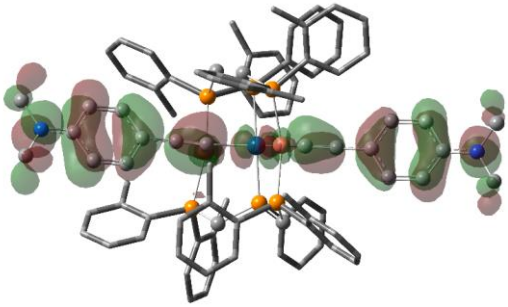

Fig. S17 The plots of HOMO and LUMO involved in the absorption (S_0) and emission (T_1) transitions for complex **4b** in the CH_2Cl_2 calculated by TD-DFT method at the PBE1PBE level (isovalue = 0.02).

	S_1	T_1
1a	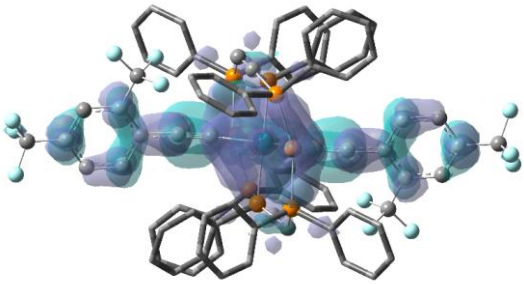	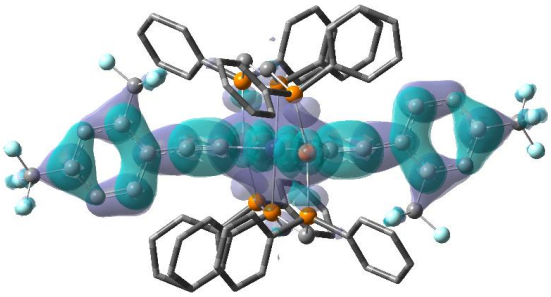
1b	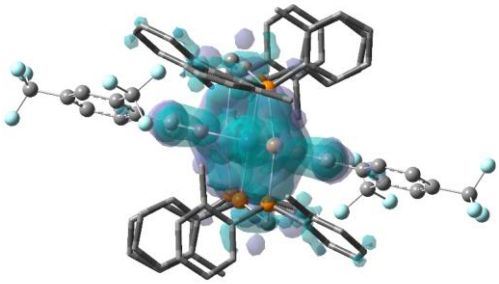	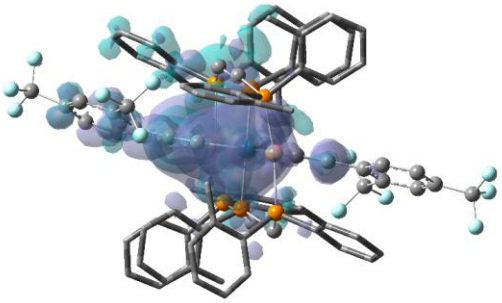

Fig. S18 The plots of the S_1 and T_1 transition orbital distribution (isovalue = 0.0004) for complexes **1a** and **1b** by TD-DFT method at the PBE1PBE level. The blue-green represents electron depletion (ED) region, while the purple stands for electron accumulation (EA) region. For clarity, the H atoms are omitted.

	S_1	T_1
2a	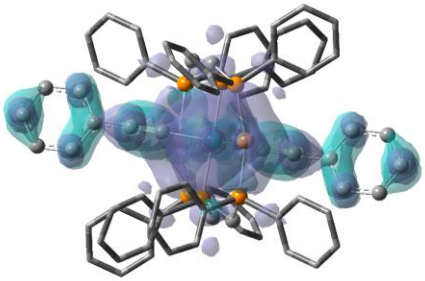	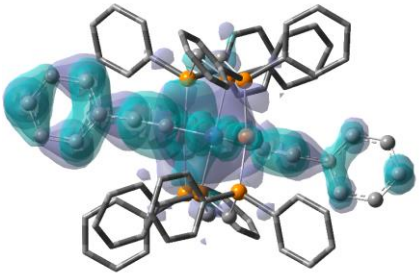
2b	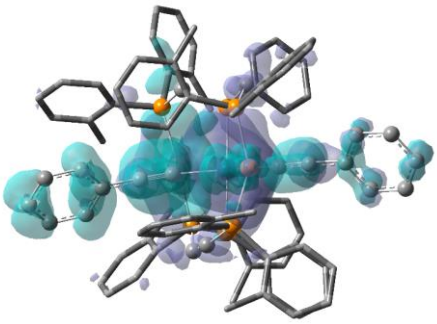	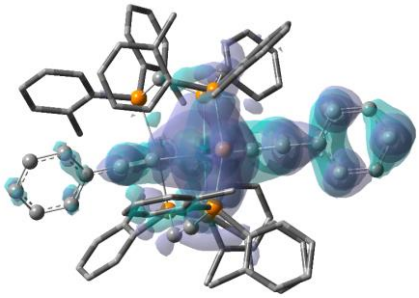

Fig. S19 The plots of the S_1 and T_1 transition orbital distribution (isovalue = 0.0004) for complexes **2a** and **2b** by TD-DFT method at the PBE1PBE level. The blue-green represents electron depletion (ED) region, while the purple stands for electron accumulation (EA) region. For clarity, the H atoms are omitted.

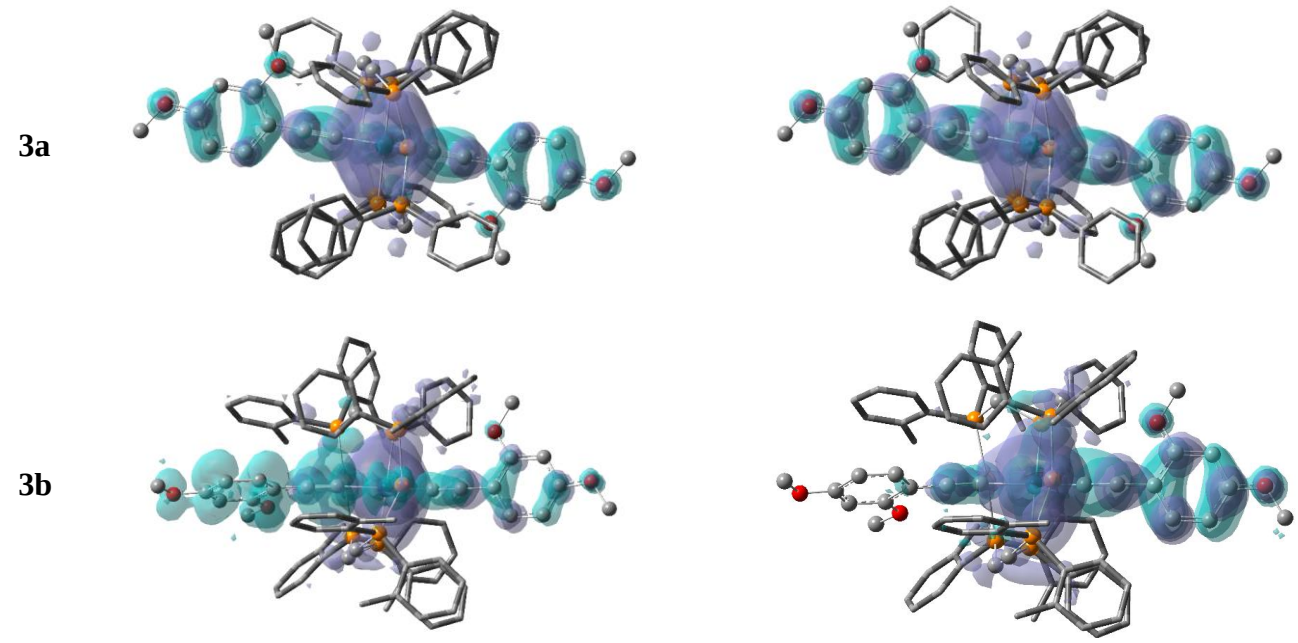

Fig. S20 The plots of the S_1 and T_1 transition orbital distribution (isovalue = 0.0004) for complexes **3a** and **3b** by TD-DFT method at the PBE1PBE level. The blue-green represents electron depletion (ED) region, while the purple stands for electron accumulation (EA) region. For clarity, the H atoms are omitted.

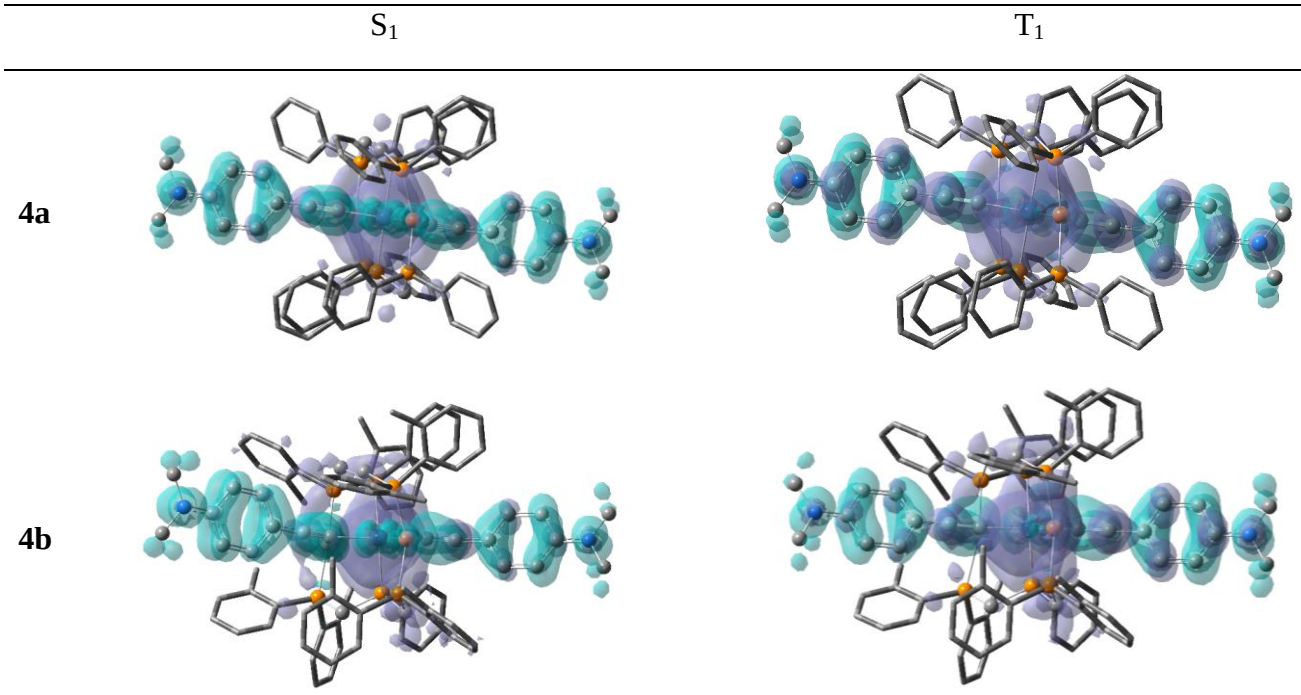

Fig. S21 The plots of the S_1 and T_1 transition orbital distribution (isovalue = 0.0004) for complexes **4a** and **4b** by TD-DFT method at the PBE1PBE level. The blue-green represents electron depletion (ED) region, while the purple stands for electron accumulation (EA) region. For clarity, the H atoms are omitted.

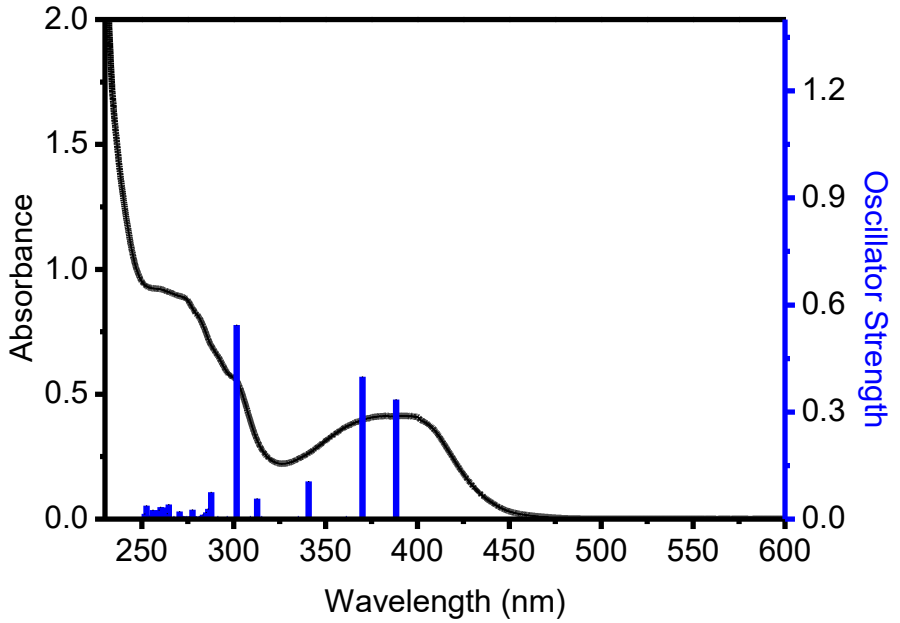

Fig. S22 The measured (line) and calculated (bar) UV-Vis absorption spectra of complex **1a**.

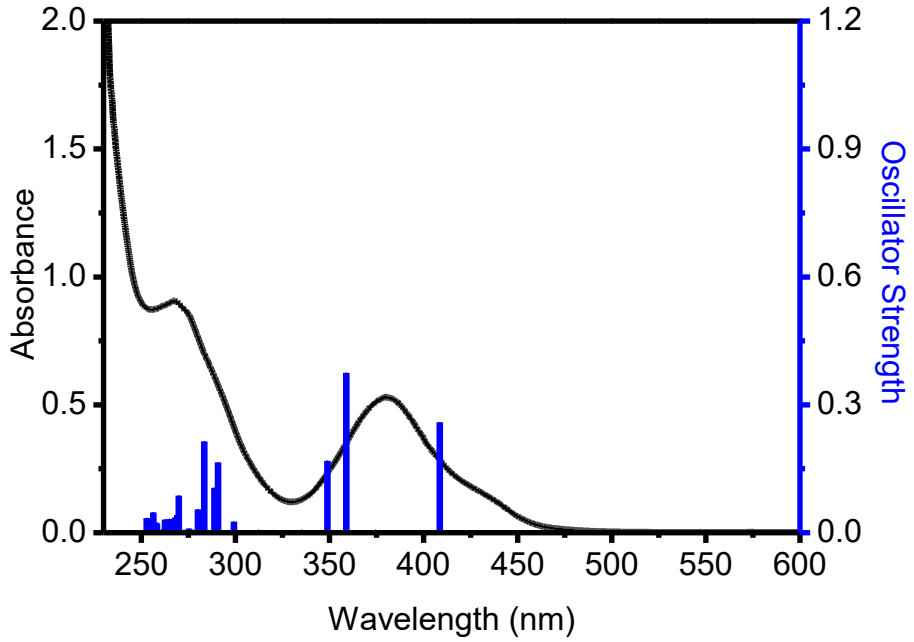

Fig. S23 The measured (line) and calculated (bar) UV-Vis absorption spectra of complex **2a**.

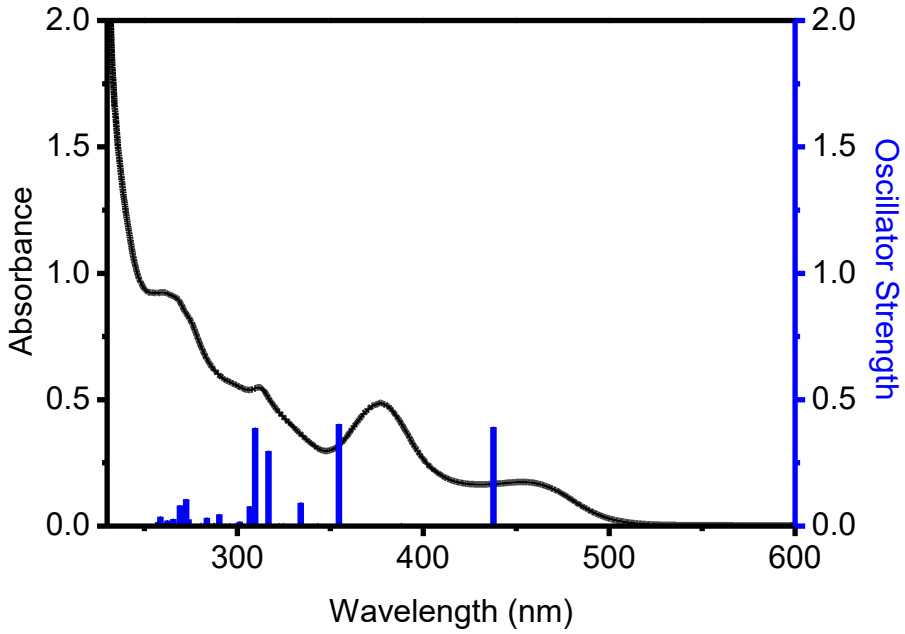

Fig. S24 The measured (line) and calculated (bar) UV-Vis absorption spectra of complex **3a**.

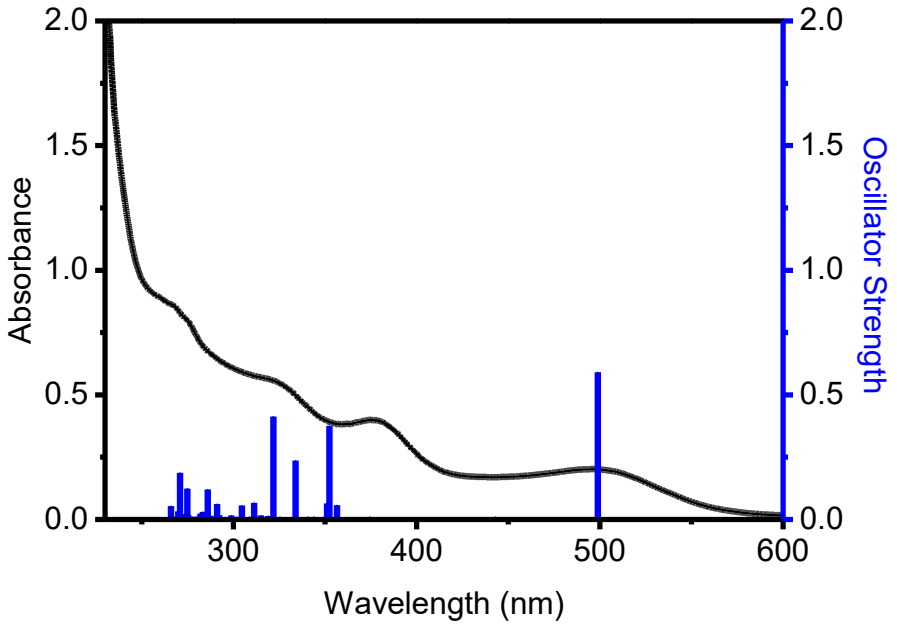

Fig. S25 The measured (line) and calculated (bar) UV-Vis absorption spectra of complex **4a**.

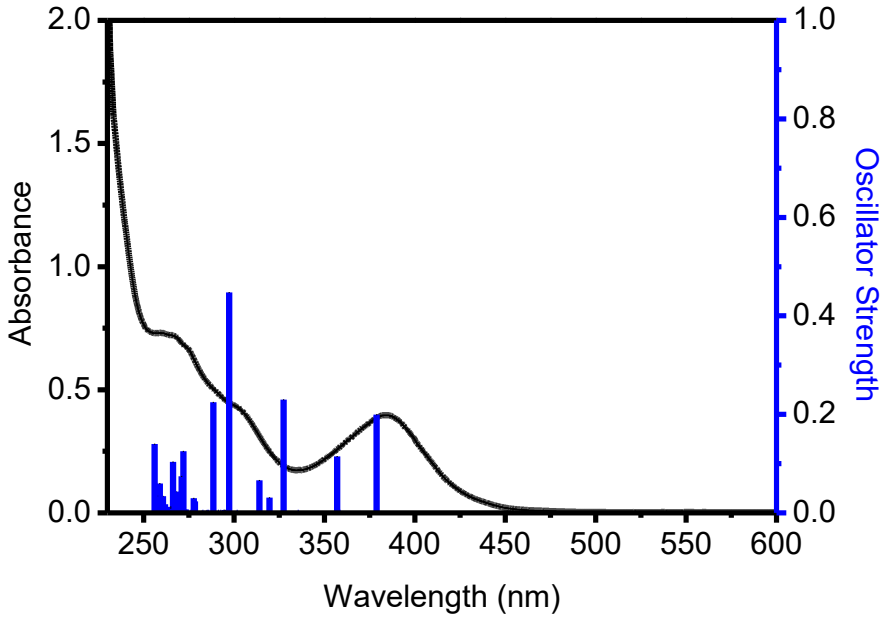

Fig. S26 The measured (line) and calculated (bar) UV-Vis absorption spectra of complex **1b**.

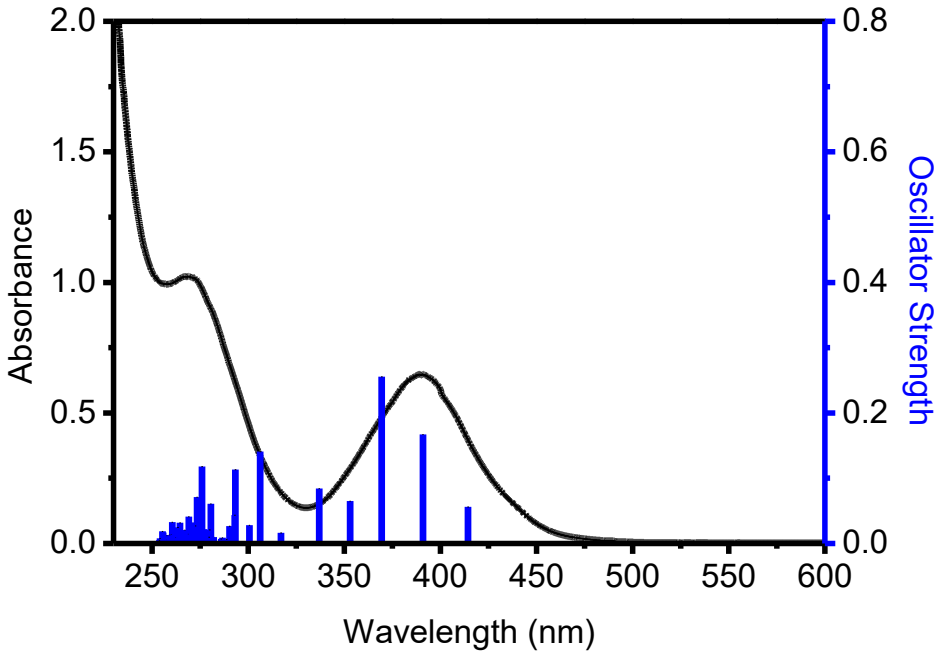

Fig. S27 The measured (line) and calculated (bar) UV-Vis absorption spectra of complex **2b**.

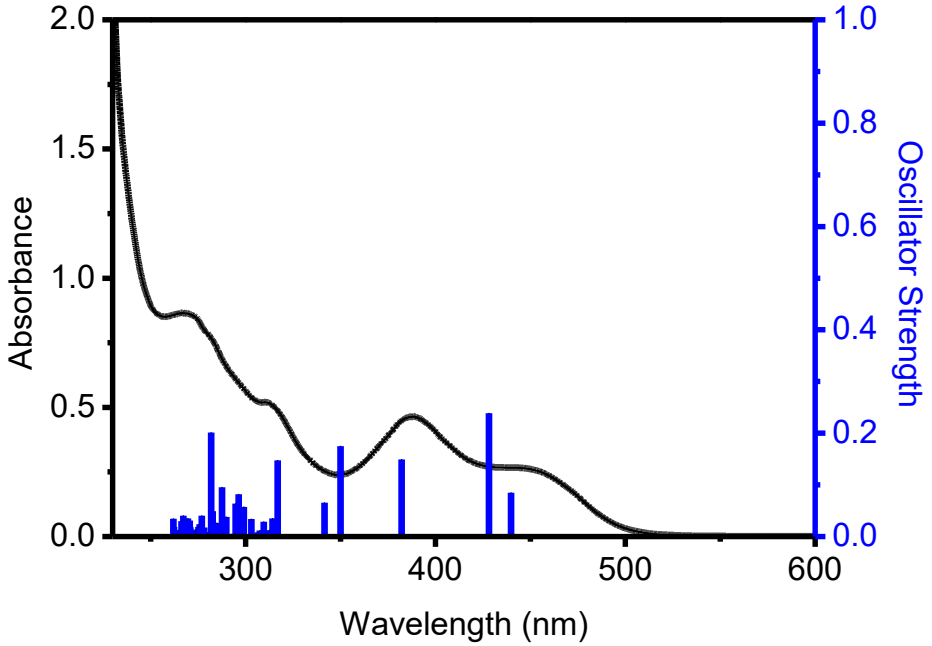

Fig. S28 The measured (line) and calculated (bar) UV-Vis absorption spectra of complex **3b**.

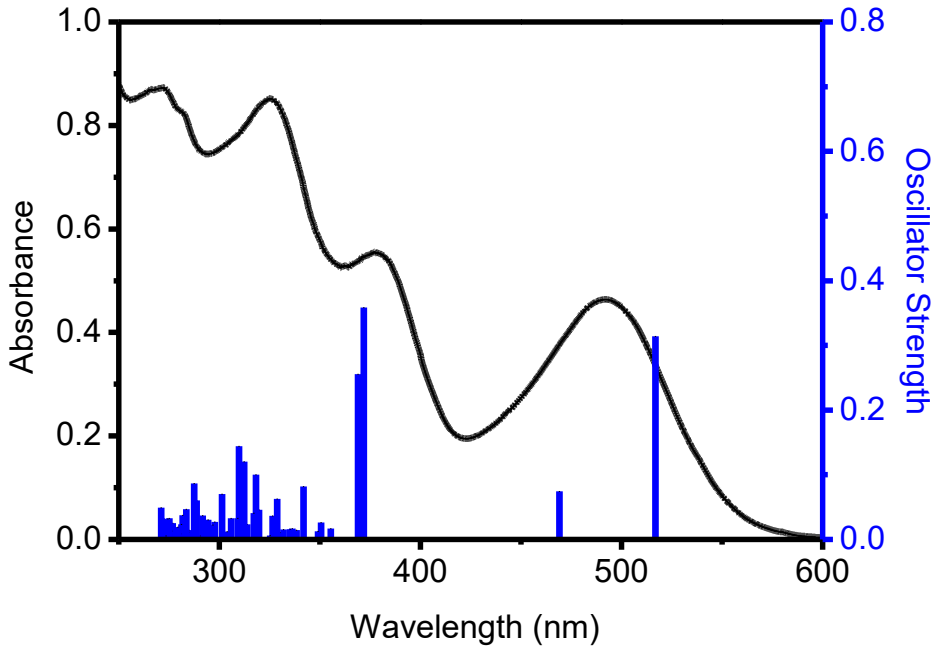

Fig. S29 The measured (line) and calculated (bar) UV-Vis absorption spectra of complex **4b**.